12

Other Properties of Solvents, Solutions, and Products Obtained from Solutions

12.1 RHEOLOGICAL PROPERTIES, AGGREGATION, PERMEABILITY, MOLECULAR STRUCTURE, CRYSTALLINITY, AND OTHER PROPERTIES AFFECTED BY SOLVENTS

George Wypych
ChemTec Laboratories, Inc., Toronto, Canada

12.1.1 RHEOLOGICAL PROPERTIES

The modification of rheological properties is one of the main reasons for adding solvents to various formulations. Rheology is also a separate complex subject which requires an in-depth understanding that can only be accomplished by consulting specialized sources such as monographic books on rheology fundamentals.[1-3] Rheology is such a vast subject that the following discussion will only outline some of the important effects of solvents.

When considering the viscosity of solvent mixtures, solvents can be divided into two groups: interacting and non-interacting solvents. The viscosity of a mixture of non-interacting solvents can be predicted with good approximation by a simple additive rule rule:

$$\log\eta = \sum_{i=1}^{i=n} \phi_i \log\eta_i \qquad [12.1.1]$$

where:

η	viscosity of solvent mixture
i	iteration subscript for mixture components (i = 1, 2, 3, ..., n)
ϕ	fraction of component i
η_i	viscosity of component i.

Interacting solvents contain either strong polar solvents or solvents which have the ability to form hydrogen bonds or influence each other on the basis of acid-base interaction. Solvent mixtures are complicated because of the changes in interaction that occurs with changes in the concentration of the components. Some general relationships describe vis-

cosity of such mixtures but none is sufficiently universal to replace measurement. Further details on solvent mixtures are included in Chapter 9.

The addition of solute(s) further complicates rheology because in such mixtures solvents may not only interact among themselves but also with the solute(s). There are also interactions between solutes and the effect of ionized species with and without solvent participation. Only very dilute solutions of low molecular weight substances exhibit Newtonian viscosity. In these solutions, viscosity is a constant, proportionality factor of shear rate and shear stress. The viscosity of these solutions is usually well described by the classical, Einstein's equation:

$$\eta = \eta_s(1 + 2.5\phi) \qquad [12.1.2]$$

where:

η_s	solvent viscosity
ϕ	volume fraction of spheres (e.g. suspended filler) or polymer fraction

If ϕ is expressed in solute mass concentration, the following relationship is used:

$$\phi = \frac{NVc}{M} \qquad [12.1.3]$$

where:

N	Avogadro's number
V	molecular volume of solute ($(4/3)\pi R^3$) with R - radius
c	solute mass concentration
M	molecular weight

Combination of equations [12.1.2] and [12.1.3] gives:

$$\frac{\eta - \eta_s}{\eta_s c} = \frac{2.5NV}{M} \qquad [12.1.4]$$

The results of studies of polymer solutions are most frequently expressed in terms of intrinsic, specific, and relative viscosities and radius of gyration; the mathematical meaning of these and the relationships between them are given below:

$$[\eta] = \lim_{c \to 0}\left(\frac{\eta - \eta_s}{\eta_s c}\right) \qquad [12.1.5]$$

$$\frac{\eta_{sp}}{c} = [\eta] + k_1[\eta]^2 c + \cdots \qquad [12.1.6]$$

$$\frac{\ln \eta_r}{c} = [\eta] - k_1'[\eta]^2 c + \cdots \qquad [12.1.7]$$

$$\eta_r = \eta_{sp} + 1 = \frac{\eta}{\eta_s} \qquad [12.1.8]$$

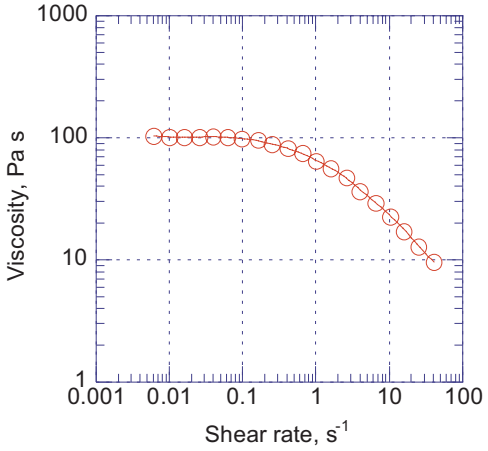

Figure 12.1.1. Viscosity vs. shear rate for 10% solution of polyisobutylene in pristane. [Data from C R Schultheisz, G B McKenna, Antec '99, SPE, New York, 1999, p 1125.]

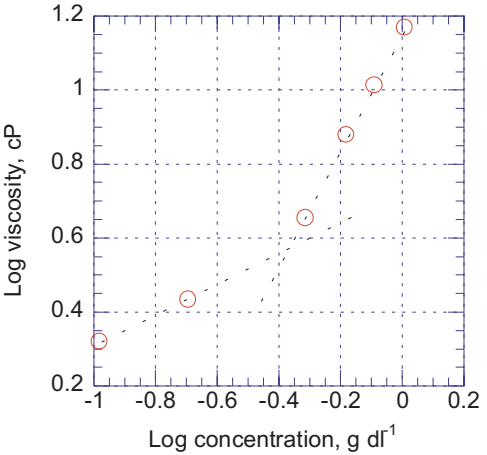

Figure 12.1.2. Viscosity of polyphenylene solution in pyrilidinone. [Data from F. Motamedi, M Isomaki, M S Trimmer, Antec '98, SPE, Atlanta, 1998, p. 1772.]

where:

$[\eta]$	intrinsic viscosity
η_{sp}	specific viscosity
η_r	relative viscosity
k_1	coefficient of direct interactions between pairs of molecules
k_1'	coefficient of indirect (hydrodynamic) interactions between pairs of molecules

In Θ solvents, the radius of gyration of unperturbed Gaussian chain enters the following relationship:

$$[\eta]_0 = \frac{\Phi_0 R_{g,0}^3}{M} \qquad [12.1.9]$$

where:

Φ_0	coefficient of intramolecular hydrodynamic interactions = $3.16 \pm 0.5 \times 10^{24}$
$R_{g,0}$	radius of gyration of unperturbed Gaussian chain

In good solvents, the expansion of chains causes an increase of viscosity as described by the following equation:

$$[\eta] = \frac{\Phi_0 \alpha_\eta^3 R_{g,0}^3}{M} \qquad [12.1.10]$$

where:

α_η	$= [\eta]^{1/3} / [\eta]_0^{1/3}$ is and effective chain expansion factor.

Existing theories are far from being universal and precise in prediction of experimental data. A more complex treatment of measurement data is needed to obtain characteristics of these "rheological" liquids.

Figure 12.1.1 shows that the viscosity of a solution depends on shear rate. These data comes from the development of a standard for instrument calibration by NIST to improve

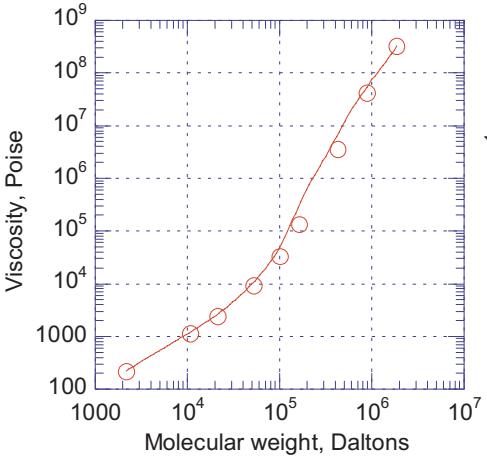

Figure 12.1.3. Viscosity of 40% polystyrene in di-2-ethyl hexyl phthalate. [Data from G D J Phillies, *Macromolecules*, **28**, No.24, 8198-208 (1995).]

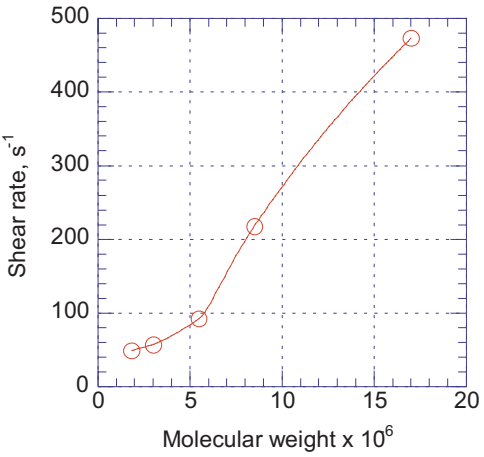

Figure 12.1.4. Shear rate of polystyrene in DOP vs. molecular weight. [Data from M Ponitsch, T Hollfelder, J Springer, *Polym. Bull.*, **40**, No.2-3, 345-52 (1998).]

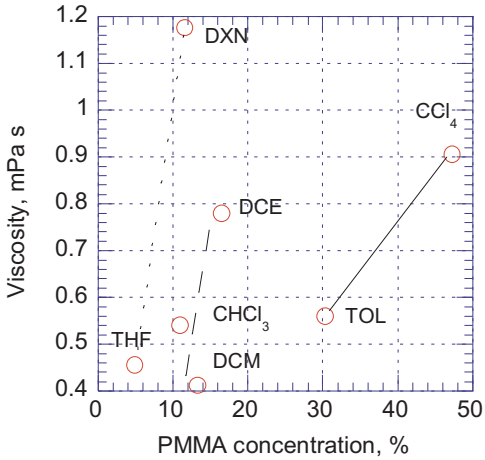

Figure 12.1.5. Viscosity of PMMA solutions in different solvents vs. PMMA concentration. Basic solvents: tetrahydrofuran, THF, and dioxane, DXN; neutral: toluene, TOL and CCl_4; acidic: 1,2-dichloroethane, DCE, $CHCl_3$, and dichloromethane, DCM. [Adapted, by permission, from M L Abel, M M Chehimi, *Synthetic Metals*, **66**, No.3, 225-33 (1994).]

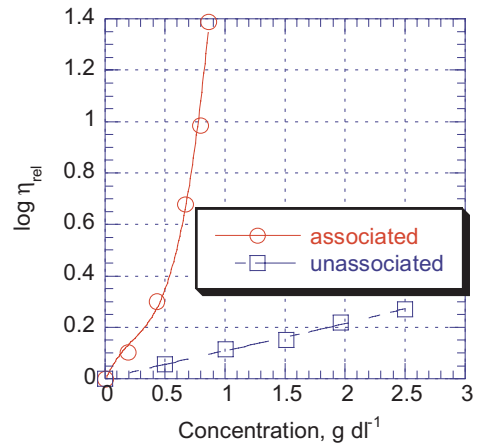

Figure 12.1.6. Relative viscosity of block copolymers with and and without segments capable of forming complexes vs. concentration. [Data from I C De Witte, B G Bogdanov, E J Goethals, *Macromol. Symp.*, **118**, 237-46 (1997).]

the accuracy of measurements by application of nonlinear liquid standards.[4] Figure 12.1.2 shows the effect of polymer concentration on the viscosity of a solution of polyphenylene in N-methyl pyrilidinone.[5] Two regimes are clearly visible. The regimes are divided by a critical concentration above which viscosity increases more rapidly due to the interaction of chains leading to aggregate formation. These two sets of data show that there

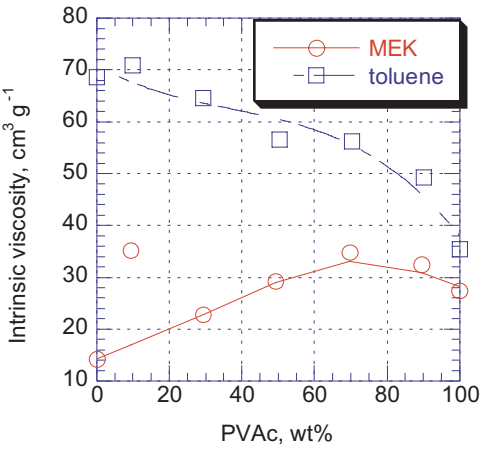

Figure 12.1.7. Intrinsic viscosity of PS/PVAc mixtures in methyl-ethyl-ketone, MEK, and toluene. [Data from H Raval, S Devi, *Angew. Makromol. Chem*., **227**, 27-34 (1995).]

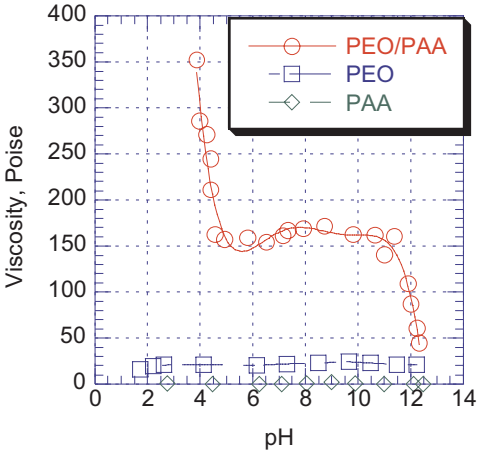

Figure 12.1.8. Viscosity of poly(ethylene oxide), PEO, poly(acrylic acid), PAA, and their 1:1 mixture in aqueous solution vs. pH. [Adapted, by permission, from I C De Witte, B G Bogdanov, E J Goethals, *Macromol. Symp*., **118**, 237-46 (1997).

are considerable departures from the simple predictions of the above equations because, based on them, viscosity should be a simple function of molecular weight. Figure 12.1.3 shows, in addition, that the relationship between viscosity of the solution and molecular weight is nonlinear.[6] Also, the critical shear rate, at which aggregates are formed, is a nonlinear function of molecular weight (Figure 12.1.4).[7]

These departures from simple relationships are representative of simple solutions. The relationships for viscosities of solution become even more complex if stronger interactions are included, such as the presence of different solvents, the presence of interacting groups within polymer, combinations of polymers, or the presence of electrostatic interactions between ionized structures within the same or different chains. Figure 12.1.5 gives one example of complex behavior of a polymer in solution. The viscosity of PMMA dissolved in different solvents depends on concentration but there is not one consistent relationship (Figure 12.1.5). Instead, three separate relationships exist each for basic, neutral, and acid solvents, respectively. This shows that solvent acid-base properties have a very strong influence on viscosity.

Figure 12.1.6 shows two different behaviors for unassociated and associated block copolymers. The first type has a linear relationship between viscosity and concentration whereas with the second there is a rapid increase in viscosity as concentration increases. This is the best described as a power law function.[8] Two polymers in combination have different reactions when dissolved in different solvents (Figure 12.1.7). In MEK, intrinsic viscosity increases as polymer concentration increases. In toluene, intrinsic viscosity decreases as polymer concentration increases.[9] The polymer-solvent interaction term for MEK is very small (0.13) indicating a stable compatible system. The interaction term for toluene is much larger (0.58) which indicates a decreased compatibility of polymers in toluene and lowers viscosity of the mixture. Figure 12.1.8 explicitly shows that the behavior of

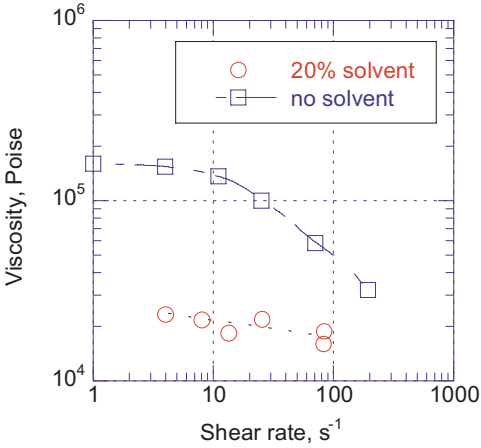

Figure 12.1.9. Apparent melt viscosity of original PET and PET containing 20% 1-methyl naphthalene vs. shear rate. [Adapted, by permission, from S Tate, S Chiba, K Tani, *Polymer*, **37**, No.19, 4421-4 (1996).]

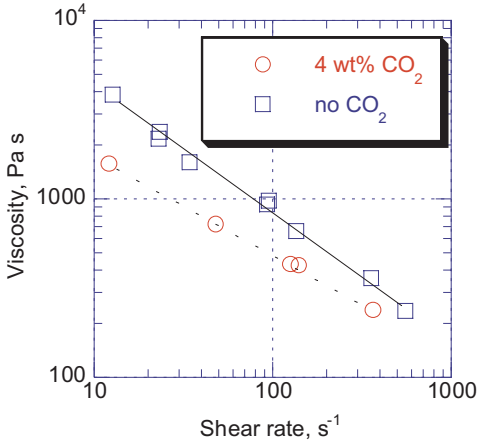

Figure 12.1.10. Viscosity behavior of PS with and without CO_2. [Data from M Lee, C Tzoganikis, C B Park, Antec '99, SPE, New York, 1999, p 2806.]

individual polymers does not necessarily have a bearing on the viscosity of their solutions. Both poly(ethylene oxide) and poly(propylene oxide) are not affected by solution pH but, when used in combination, they become sensitive to solution pH. A rapid increase of viscosity at a lower pH is ascribed to intermolecular complex formation. This behavior can be used for thickening of formulations.[8]

Figures 12.1.9 and 12.1.10 show one potential application in which a small quantity of solvents can be used to lower melt viscosity during polymer processing. Figure 12.1.9 shows that not only can melt viscosity be reduced but also that the viscosity is almost independent of shear rate.[10] In environmentally friendly process supercritical fluids can be used to reduce melt viscosity.

The above data illustrate that the real behavior of solutions is much more complex than it is intuitively predicted based on simple models and relationships. The proper selection of solvent can be used to tailor the properties of formulation to the processing and application needs. Solution viscosity can be either increased or decreased to meet process technology requirements or to give the desired material properties.

REFERENCES

1 A Ya Malkin, **Rheology Fundamentals**, *ChemTec Publishing*, Toronto, 1994.
2 Ch W Macosko, **Rheology. Principles, Measurements, and Applications**, *VCH Publishers*, New York, 1994.
3 R I Tanner, K. Walters, **Rheology: an Historical Perspective**, *Elsevier*, Amsterdam, 1998.
4 C R Schultheisz, G B McKenna, Antec '99, SPE, New York, 1999, p 1125.
5 F Motamedi, M Isomaki, M S Trimmer, Antec '98, SPE, Atlanta, 1998, p. 1772.
6 G D J Phillies, *Macromolecules*, **28**, No.24, 8198-208 (1995).
7 M Ponitsch, T Hollfelder, J Springer, *Polym. Bull.*, **40**, No.2-3, 345-52 (1998).
8 I C De Witte, B G Bogdanov, E J Goethals, *Macromol. Symp.*, **118**, 237-46 (1997).
9 H Raval, S Devi, *Angew. Makromol. Chem.*, **227**, 27-34 (1995).

10 S Tate, S Chiba, K Tani, *Polymer*, 37, No.19, 4421-4 (1996).
11 M L Abel, M M Chehimi, *Synthetic Metals*, **66**, No.3, 225-33 (1994).
12 M Lee, C Tzoganikis, C B Park, Antec '99, SPE, New York, 1999, p 2806.

12.1.2 AGGREGATION

The development of materials with an engineered morphological structure, such as selective membranes and nanostructures, employs principles of aggregation in these interesting technical solutions. Here, we consider some basic principles of aggregation, methods of studies, and outcomes. The discipline is relatively new therefore for the most part, only exploratory findings are available now. The theoretical understanding is still to be developed and this development is essential for the control of industrial processes and development of new materials.

Methods of study and data interpretation still require further work and refinement. Several experimental techniques are used, including: microscopy (TEM, SEM);[1,2] dynamic light scattering[3-6] using laser sources, goniometers, and digital correlators; spectroscopic methods (UV, CD, fluorescence);[7,8] fractionation; solubility and viscosity measurements;[9] and acid-base interaction.[10]

Dynamic light scattering is the most popular method. Results are usually expressed by the radius of gyration, R_g, the second viral coefficient, A_2, the association number, p, and the number of arms, f, for starlike micelles.

Zimm's plot and equation permits R_g and A_2 to be estimated:

$$\frac{KC}{R_\theta} = \frac{1}{\overline{M}_w}\left[1 + \frac{16}{3}\pi^2 \frac{R_g^2}{\lambda_0^2}\sin^2\theta + \cdots\right] + 2A_2C + \cdots \qquad [12.1.11]$$

where:

K	optical constant
C	polymer concentration
R_θ	Rayleigh ratio for the solution
$\overline{M}_w$	weight average molecular weight
λ_0	wavelength of light
θ	scattering angle.

The following equations are used to calculate p and f:

$$p = \frac{M_{agg}}{M_1}; M_{agg} = KI_{q\to 0} / C \qquad [12.1.12]$$

$$\frac{R_g}{R_{garm}} = f^{(1-v)/2} \qquad [12.1.13]$$

where:

M_{agg}	mass of aggregates
M_1	mass of free copolymers
I	scattered intensity
R_{garm}	radius of gyration of linear polymer
v	excluded volume exponent.

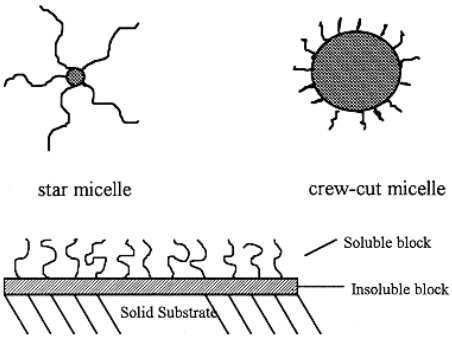

Figure 12.1.11. Morphological features: starlike and crew-cut. The bottom drawing illustrates polymer brush. [Adapted, by permission from G Liu, *Macromol. Symp*., **113**, 233 (1997).]

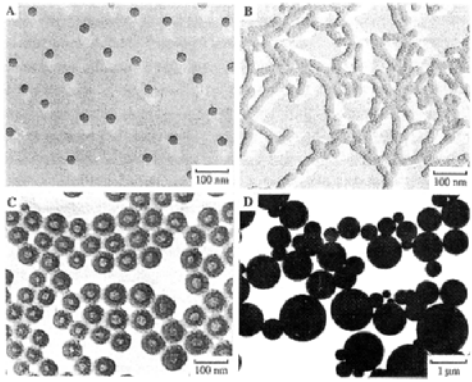

Figure 12.1.12. Morphological features of PS-PAA copolymer having different ratios of PS and PAA block lengths: A - 8.3, B- 12, C - 20.5, and D - 50. [Adapted, by permission, from L Zhang, A Eisenberg, *Macromol. Symp*., **113**, 221-32 (1997).]

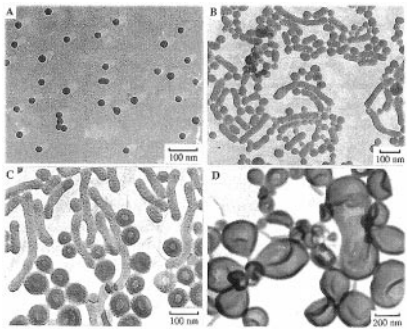

Figure 12.1.13. PS-PAA aggregates of different morphologies depending on its concentration in DMF: A - 2, B - 2.6, C - 3, D - 4 wt%. [Adapted, by permission, from L Zhang, A Eisenberg, *Macromol. Symp*., **113**, 221-32 (1997).]

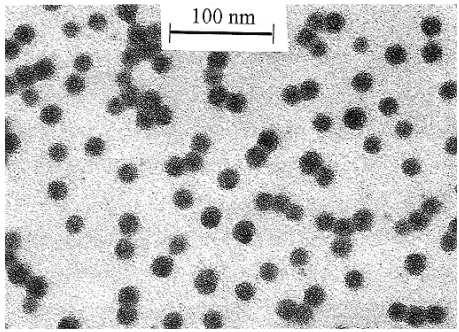

Figure 12.1.14. TEM micrograph of nanospheres. [Adapted, by permission, from G Liu, *Macromol. Symp*., **113**, 233 (1997).]

Three major morphological features are under investigation: starlike, crew-cut, and polymer brushes (Figure 12.1.11). Morphological features have been given nick-names characterizing the observed shapes, such as “animals” or “flowers” to distinguish between various observed images.[6] Figure 12.1.12 shows four morphologies of aggregates formed by polystyrene, PS,-poly(acrylic acid), PAA, diblock copolymers.[1] The morphology produced was a direct result of the ratio between lengths of blocks of PS and PAA (see Figure 12.1.12). When this ratio is low (8.3), spherical micelles are formed. With a slightly higher ratio (12), rod-like micelles result which have narrow distribution of diameter but variable length. Increasing ratio even further (20.5) causes vesicular aggregates to form. With the highest ratio (50), large spherical micelles are formed. One of the reasons for the differences in these formations is that the surface tension between the core and the solvent varies widely. In order to decrease interfacial tension between the core and the solvent, the aggregate increases the core size.[1] Polymer concentration in solution also affects aggregate for-

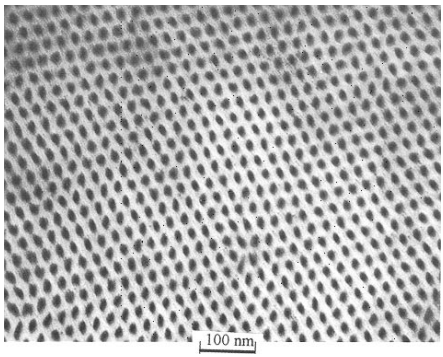

Figure 12.1.15. TEM micrograph of assemblies of cylindrical aggregates. [Adapted, by permission, from G Liu, *Macromol. Symp*., **113**, 233 (1997).]

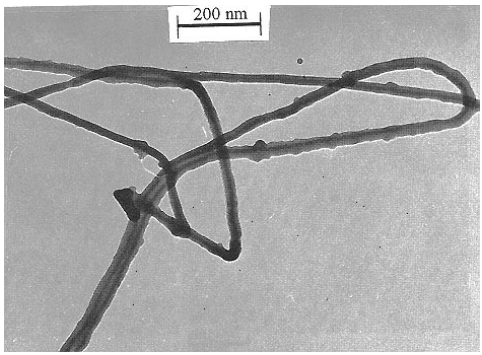

Figure 12.1.16. TEM micrograph of nanofibers. [Adapted, by permission, from G Liu, *Macromol. Symp*., **113**, 233 (1997).]

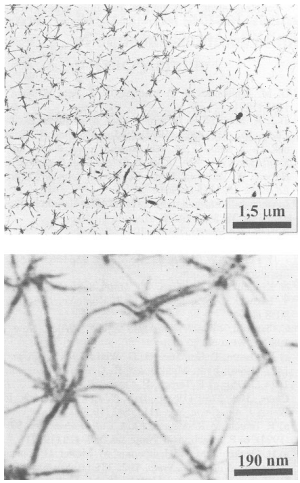

Figure 12.1.17. TEM micrograph of knots and strands formed in carbohydrate amphiphile. [Adapted, by permission, from U Beginn, S Keinath, M Moller, *Macromol. Chem. Phys*., **199**, No.11, 2379-84 (1998).]

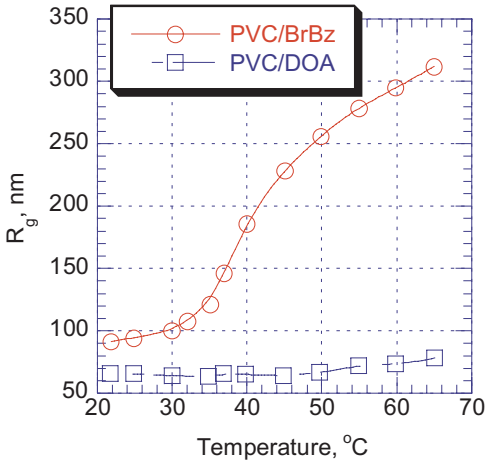

Figure 12.1.18. Radius of gyration vs. temperature for PVC solutions in bromobenzene, BrBz, and dioxane, DOA. [Adapted, by permission, from Hong Po-Da, Chen Jean-Hong Chen, *Polymer*, **40**, 4077-4085, (1999).]

mation as Figure 12.1.13 shows. As polymer concentration increases, spherical micelles are replaced by a mixture of rod-like structures and vesicles. With a further increase in concentration, the rod-like shapes disappear and only vesicles remain.

Figures 12.1.14-12.1.16 show a variety of shapes which have been observed. These include nanospheres, assemblies of cylindrical aggregates, and nanofibers.[11] Nanospheres were obtained by the gradual removal of solvent by dialysis, fibers were produced by a series of processes involving dissolution, crosslinking, and annealing. Figure 12.1.17 sheds some light on the mechanism of aggregate formation. Two elements are clearly visible from micrographs: knots and strands. Based on studies of carbohydrate amphiphiles, it is concluded that knots are formed early in the process by spinodal decomposition. Formation of

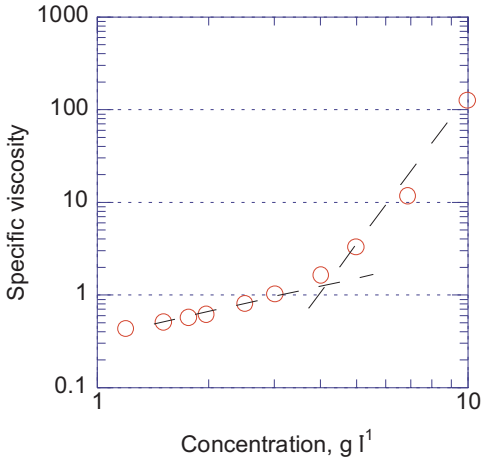

Figure 12.1.19. Specific viscosity of PVC in bromobenzene solution vs. concentration. [Adapted, by permission, from Hong Po-Da, Chen Jean-Hong Chen, *Polymer*, **40**, 4077-4085, (1999).]

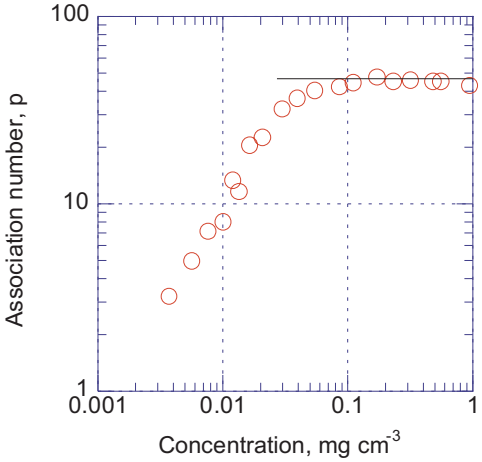

Figure 12.1.20. Diblock copolymer association number vs. its concentration. [Adapted, by permission, from D Lairez, M Adam, J-P Carton, E Raspaud, *Macromolecules*, **30**, No.22, 6798-809 (1997).]

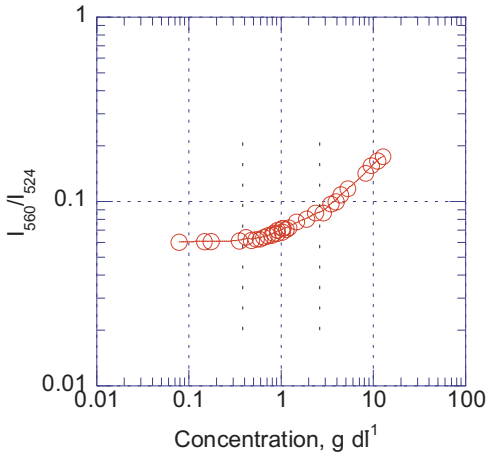

Figure 12.1.21. Fluorescence intensity ratio vs. concentration of polyimide in chloroform. [Data from H Luo, L Dong, H Tang, F Teng, Z Feng, *Macromol. Chem. Phys*., **200**, No.3, 629-34 (1999).]

strands between knots occurs much later.[2] A similar course of events occurs with the molecular aggregation of PVC solutions.[5]

Figure 12.1.18 gives more details on the mechanism of aggregate formation.[5] PVC dissolved in bromobenzene, BrBz, undergoes a coil to globule transition which does not occur in dioxane, DOA, solution. Bromobenzene has a larger molar volume than dioxane and the polymer chain must readjust to the solvent molar volume in order to interact. Figure 12.1.19 shows that two regimes of aggregation are involved which are divided by a certain critical value. Below the critical value chains are far apart and do not interact due to contact self-avoidance. At the critical point, knots, similar to shown in Figure 12.1.17, begin to form and the resultant aggregation increases viscosity. As the polymer concentration increases, the association number, p, also increases, but then levels off (Figure 12.1.20).

Fluorescence studies (Figure 12.1.21) show that there are two characteristic points relative to concentration. Below the first point, at 0.13 g/dl, in very dilute solution, molecules are highly expanded and distant from one another and fluorescence does not change. Between the two points, individual chain coils begin to sense each other and become affected

by the presence of neighbors forming intermolecular associations. Above the second point, coils begin to overlap leading to dense packing.[8] These data are essentially similar to those presented in Figure 12.1.20 but cover a broader concentration range.

The above studies show that there are many means of regulating aggregate size and shape which is likely to become an essential method of modifying materials by morphological engineering.

REFERENCES

1 L Zhang, A Eisenberg, *Macromol. Symp*., **113**, 221-32 (1997).
2 U Beginn, S Keinath, M Moller, *Macromol. Chem. Phys*., **199**, No.11, 2379-84 (1998).
3 P A Cirkel, T Okada, S Kinugasa, *Macromolecules*, **32**, No.2, 531-3 (1999).
4 K Chakrabarty, R A Weiss, A Sehgal, T A P Seery, *Macromolecules*, **31**, No.21, 7390-7 (1998).
5 Hong Po-Da, Chen Jean-Hong Chen, *Polymer*, **40**, 4077-4085, (1999).
6 D Lairez, M Adam, J-P Carton, E Raspaud, *Macromolecules*, **30**, No.22, 6798-809 (1997).
7 R Fiesel, C E Halkyard, M E Rampey, L Kloppenburg, S L Studer-Martinez, U Scherf, U H F Bunz, *Macromol. Rapid Commun*., **20**, No.3, 107-11 (1999).
8 H Luo, L Dong, H Tang, F Teng, Z Feng, *Macromol. Chem. Phys*., **200**, No.3, 629-34 (1999).
9 A Leiva, L Gargallo, D Radic, *J. Macromol. Sci. B*, **37**, No.1, 45-57 (1998).
10 S Bistac, J Schultz, *Macromol. Chem. Phys*., **198**, No. 2, 531-5 (1997).
11 G Liu, *Macromol. Symp*., **113**, 233 (1997).

12.1.3 PERMEABILITY

The phenomenon of solvent transport through solid barriers has three aspects which discussed under the heading of permeability. These are the permeation of solvent through materials (films, containers, etc.); the use of pervaporation membranes to separate organic solvents from water or water from solvents; the manufacture of permeate selective membranes.

The permeability of different polymers and plastics to various solvents can be found in an extensive, specialized database published as a book and as a CD-ROM.[1] The intrinsic properties of polymers can be modified in several ways to increase their resistance and reduce their permeability to solvents. The development of plastic gas tanks was a major driving force behind these developments and now various plastic containers are manufactured using similar processes.

Fluorination of plastics, usually polypropylene or polyethylene, is by far the most common modification. Containers are typically manufactured by a blow molding process where they are protected by a fluorination process applied on line or, more frequently, off line. The first patent[2] for this process was issued in 1975 and numerous other patents, some of them issued quite recently have made further improvements to the process.[3] The latest processes use a reactive gas containing 0.1 to 1% fluorine to treat parison within the mold after it was expanded.[3] Containers treated by this process are barrier to polar liquids, hydrocarbon fuels, and carbon fuels containing polar liquids such as alcohols, ethers, amines, carboxylic acids, ketones, etc. Superior performance is achieved when a hydrogen purge precedes the exposure of the container to oxygen.

In another recent development,[4] containers are being produced from a blend of polyethylene and poly(vinylidene fluoride) with aluminum stearate as compatibilizer. This process eliminates the use of the toxic gas fluorine and by-products which reduces environmental pollution and disposal problems. It is argued that fluorinated containers may not perform effectively when the protective layer becomes damaged due to stress cracking.

Such a blend is intended as a replacement for previous blends of polyamide and polyethylene used in gas tanks and other containers. These older blends were exposed to a mixture of hydrocarbons but now oxygenated solvents (e.g., methanol) have been added which cause an unacceptable reduction of barrier properties. A replacement technology is needed. Improved barrier properties in this design[4] comes from increased crystallinity of the material brought about by controlling laminar thickness of polyethylene crystals and processing material under conditions which favor the crystallization of poly(vinylidene fluoride).

Another approach involves the use of difunctional telechelic polyolefins with ester, hydroxyl, and amine terminal groups.[5] Telechelic polyolefins can be used to make polyesters, polyamides, and polyurethanes with low permeability to solvents and gases.

Separation processes such as ultrafiltration and microfiltration use porous membranes which allow the passage of molecules smaller than the membrane pore size. Ultrafiltration membranes have pore sizes from 0.001 to 0.1 μm while microfiltration membranes have pore sizes in the range of 0.02 to 10 μm. The production of these membranes is almost exclusively based on non-solvent inversion method which has two essential steps: the polymer is dissolved in a solvent, cast to form a film then the film is exposed to a non-solvent. Two factors determine the quality of the membrane: pore size and selectivity. Selectivity is determined by how narrow the distribution of pore size is.[6,7] In order to obtain membranes with good selectivity, one must control the non-solvent inversion process so that it inverts slowly. If it occurs too fast, it causes the formation of pores of different sizes which will be non-uniformly distributed. This can be prevented either by an introduction of a large number of nuclei, which are uniformly distributed in the polymer membrane or by the use of a solvent combination which regulates the rate of solvent replacement.

Typical solvents used in membrane production include: N-methylpyrrolidinone, N,N-dimethylacetamide, N,N-dimethylformamide, dimethylsulfoxide, tetrahydrofuran, dioxane, dichloromethane, methyl acetate, ethyl acetate, and chloroform. They are used alone or in mixtures.[6] These are used most frequently as non-solvents: methanol, ethanol, 1-propanol, 2-propanol, 1-butanol, 2-butanol, and t-butanol. Polymers involved include: polysulfone, polyethersulfone, polyamide, polyimide, polyetherimide, polyolefins, polycarbonate, polyphenyleneoxide, poly(vinylidene fluoride), polyacrylonitrile, and cellulose and its derivatives.

A second method of membrane preparation is based on the thermally-induced phase separation process.[8] The goal of this process is to produce a membrane which has an ultrathin separation layer (to improve permeation flux) and uniform pores.[9] In this process, polymer is usually dissolved in a mixture of solvents which allow the mixture to be processed either by spinning or by coating. The desired membrane morphology is obtained through cooling to induce phase separation of

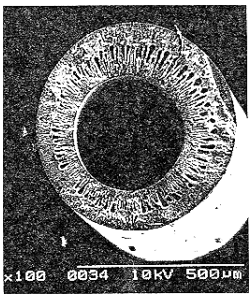

Figure 12.1.22. PEI fiber from NMP. [Adapted, by permission from D Wang, K Li, W K Teo, *J. Appl. Polym. Sci.*, **71**, No.11, 1789-96 (1999).]

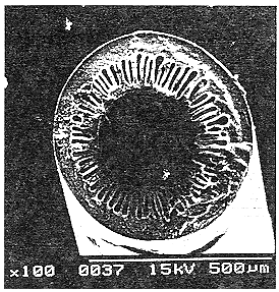

Figure 12.1.23. PEI fiber from DMF. [Adapted, by permission from D Wang, K Li, W K Teo, *J. Appl. Polym. Sci.*, **71**, No.11, 1789-96 (1999).]

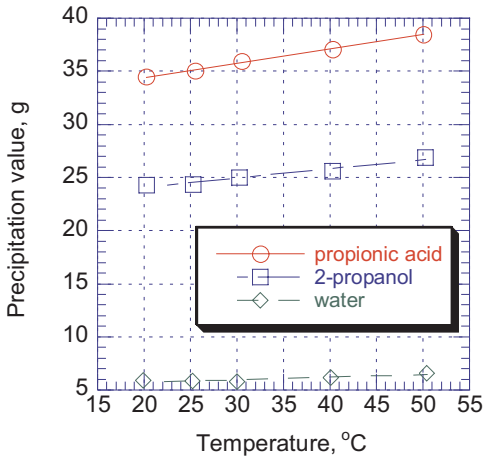

Figure 12.1.24. Precipitation value for PEI/NMP system with different non-solvents vs. temperature. [Data from D Wang, Li K, W K Teo, *J. Appl. Polym. Sci*., **71**, No.11, 1789-96 (1999).]

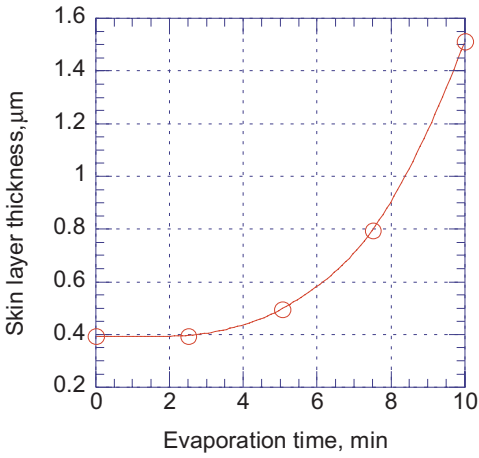

Figure 12.1.25. Skin thickness vs. evaporation time of formation of asymmetric membrane from polysulfone. [Data from A Yamasaki, R K Tyagi, A E Fouda, T Matsura, K Jonasson, *J. Appl. Polym. Sci*., **71**, No.9, 1367-74 (1999).]

polymer/solvent/non-solvent system. One practices in use is the addition of non-solvents to the casting solution.[10] The mixture should be designed such that homogeneous casting is still possible but the thermodynamic condition approaches phase separation. Because of cooling and/or evaporation of one of the solvents, demixing occurs before material enters coagulation bath.[10]

Figures 12.1.22 and 12.1.23 explain technical principles behind formation of efficient and selective membrane. Figure 12.1.22 shows a micrograph of hollow PEI fiber produced from N-methyl-2-pyrrolidone, NMP, which has thin surface layer and uniform pores and Figure 12.1.23 shows the same fiber obtained from a solution in dimethylformamide, DMF, which has a thick surface layer and less uniform pores.[9] The effect depends on the interaction of polar and non-polar components. The compatibility of components was estimated based on their Hansen's solubility parameter difference. The compatibility increases as the solubility parameter difference decreases.[9] Adjusting temperature is another method of control because the Hansen's solubility parameter decreases as the temperature increases. A procedure was developed to determine precipitation values by titration with non-solvent to a cloud point.[9] Use of this procedure aids in selecting a suitable non-solvent for a given polymer/solvent system. Figure 12.1.24 shows the results from this method.[9] Successful in membrane production by either non-solvent inversion or thermally-induced phase separation requires careful analysis of the compatibilities between polymer and solvent, polymer and non-solvent, and solvent and non-solvent. Also the processing regime, which includes temperature control, removal of volatile components, uniformity of solvent replacement must be carefully controlled.

Efforts must be made to select solvents of low toxicity and to minimize solvent consumption. An older method of producing polyetherimide membranes involved the use of a mixture of two solvents: dichloromethane (very volatile) and 1,1,2-trichloroethane together

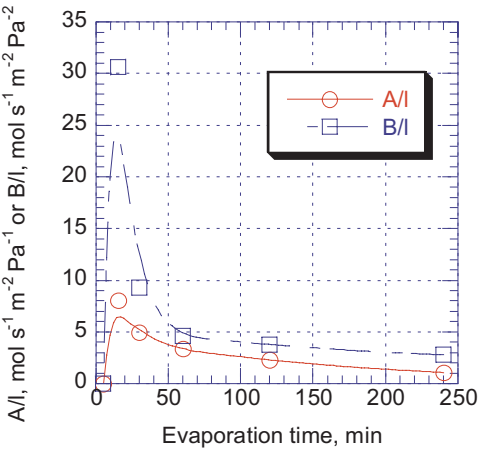

Figure 12.1.26. Pervaporation transport parameters: A/l (liquid transport) and B/l (vapor transport) vs. evaporation time during membrane preparation from aromatic polyamide. [Data from A Yamasaki, R K Tyagi, A Fouda, T Matsuura, *J. Appl. Polym. Sci*., **57**, No.12, 1473-81 (1995).]

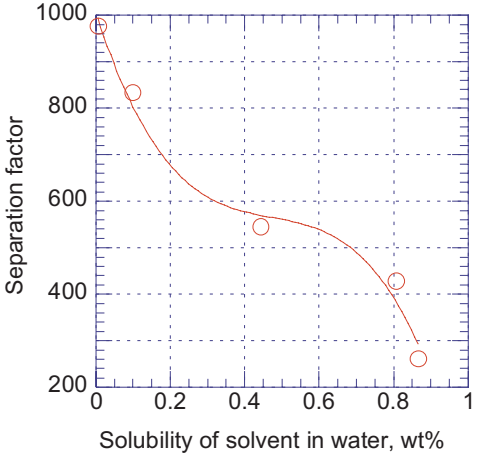

Figure 12.1.27. Separation factor vs. solubility of solvents in water. [Adapted, by permission, from M Hoshi, M Kobayashi, T Saitoh, A Higuchi, N Tsutomu, *J. Appl. Polym. Sci*., **69**, No.8, 1483-94 (1998).]

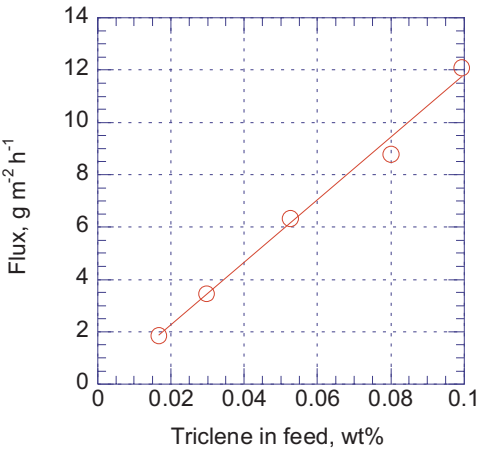

Figure 12.1.28. Effect of triclene concentration in feed solution on its pervaporation flux through acrylic membrane. [Data from M Hoshi, M Kobayashi, T Saitoh, A Higuchi, N Tsutomu, *J. Appl. Polym. Sci*., **69**, No.8, 1483-94 (1998).]

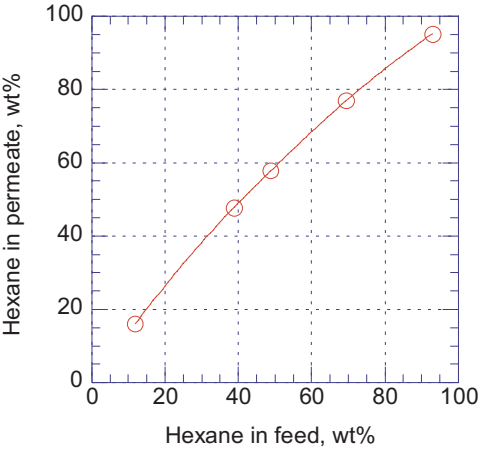

Figure 12.1.29. Effect of hexane concentration in feed solution on its concentration in permeate through acrylic membrane. [Data from M Hoshi, M Kobayashi, T Saitoh, A Higuchi, N Tsutomu, *J. Appl. Polym. Sci*., **69**, No.8, 1483-94 (1998).]

with a mixture of non-solvents: xylene and acetic acid. In addition, large amounts of acetone were used in the coagulation bath. A more recent process avoided environmental problems by using tetrahydrofuran and γ-butyrolactone in a process in which water only is used in the coagulating bath (membrane quality remained the same).[10]

Thermally-induced phase separation has been applied to the production of polysilane foams.[11] Variation of polymer concentration, solvent type, and cooling rate have been used to refine the macrostructure. Both these membrane production methods rely on the formation of aggregates of controlled size and shape as discussed in the previous section.

Figure 12.1.25 shows the effect of of solvent evaporation time on the skin layer thickness. It is only in the beginning of the process that skin thickness does not increase. Thereafter there is rapid skin thickness growth. Polymer concentration is the other important determinant of skin thickness. Figure 12.1.26 shows that during very short evaporation times (5 min), even though skin is thin the pores diameter is so small that the pervaporation parameters A/l and B/l, which characterize liquid and vapor transport, respectively, do not increase. Longer evaporation times bring about a gradual decrease in transport properties.[12,13]

Figure 12.1.27 shows the relationship between the separation factor and the solubility of solvents in water. The separation of solvent by a pervaporation membrane occurs less efficiently as solvent solubility increases.The more concentrated the solution of solvent, the faster is the separation (Figure 12.1.28). Separation of hexane from a mixture with heptane is similar (Figure 12.1.29). The acrylic membrane shows good selectivity. These examples demonstrate the usefulness of pervaporation membranes in solvent recovery processes.

REFERENCES

1 Permeability and Other Film Properties, Plastics Design Library, Norwich, 1996.
2 **US Patent 3,862,284**, 1975.
3 J P Hobbs, J F DeiTos, M Anand, **US Patent 5,770,135**, Air Products and Chemicals, Inc., 1998 and **US Patent 5,244,615**, 1992.
4 R T Robichaud, **US Patent 5,702,786**, Greif Bros. Corporation, 1997.
5 P O Nubel, H B Yokelson, **US Patent 5,731,383**, Amoco Corporation, 1998 and **US Patent 5,589,548**, 1996.
6 J M Hong, S R Ha, H C Park, Y S Kang, K H Ahn, **US Patent 5,708,040**, Korea Institute of Science and Technology, 1998.
7 K-H Lee, J-G Jegal, Y-I Park, **US Patent 5,868,975**, Korea Institute of Science and Technology, 1999.
8 J M Radovich, M Rothberg, G Washington, **US Patent 5,645,778**, Althin Medical, Inc., 1997.
9 D Wang, Li K, W K Teo, *J. Appl. Polym. Sci*., **71**, No.11, 1789-96 (1999).
10 K-V Peinemann, J F Maggioni, S P Nunes, *Polymer*, **39**, No.15, 3411-6 (1998).
11 L L Whinnery, W R Even, J V Beach, D A Loy, *J. Polym. Sci.: Polym. Chem. Ed*., **34**, No.8, 1623-7 (1996).
12 A Yamasaki, R K Tyagi, A Fouda, T Matsuura, *J. Appl. Polym. Sci*., **57**, No.12, 1473-81 (1995).
13 A Yamasaki, R K Tyagi, A E Fouda, T Matsura, K Jonasson, *J. Appl. Polym. Sci*., **71**, No.9, 1367-74 (1999).
14 M Hoshi, M Kobayashi, T Saitoh, A Higuchi, N Tsutomu, *J. Appl. Polym. Sci*., **69**, No.8, 1483-94 (1998).

12.1.4 MOLECULAR STRUCTURE AND CRYSTALLINITY

The gelation of polymer-solvent systems was initially thought of as a process which occurs only in poor solvents which promote chain-chain aggregation. Further studies have revealed that many polymers also form gels in good solvents. This has prompted research which attempts to understand the mechanisms of gelation. These efforts have contributed the current understanding of the association between molecules of solvents and polymers.[1] Studies on isotactic, iPS, and syndiotactic, sPS, polystyrenes[2-6] have confirmed that, although both polymers have the same monomeric units, they are significantly different in terms of their solubility, gelation, and crystallization. In systems where sPS has been dissolved in benzene and carbon tetrachloride, gelation is accomplished in a few minutes

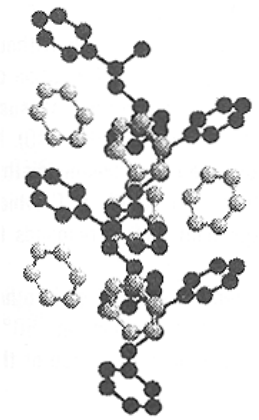

Figure 12.1.30. Molecular model of polystyrene and benzene rings alignment. [Adapted by permission, from J M Guenet, *Macromol. Symp.*, **114**, 97 (1997).]

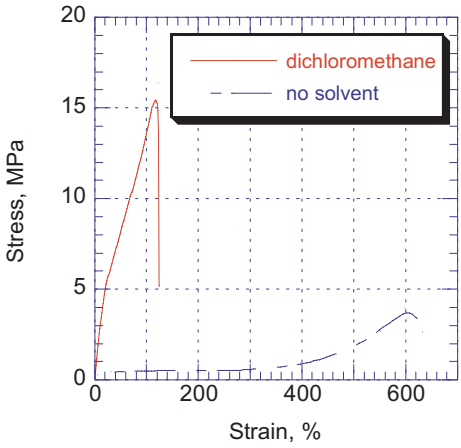

Figure 12.1.31. Stress-strain behavior at 130ºC of glassy sPS with and without immersion in dichloromethane. [Data from C Daniel, L Guadagno, V Vittoria, *Macromol. Symp.*, **114**, 217 (1997).]

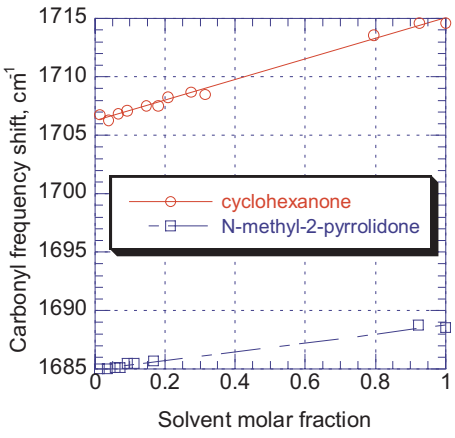

Figure 12.1.32. Carbonyl frequency vs. molar fraction of solvent. [Adapted, by permission, from J M Gomez-Elvira, P Tiemblo, G Martinez, J Milan, *Macromol. Symp.*, **114**, 151 (1997).]

whereas in chloroform it takes tens of hours. Adding a small amount of benzene to the chloroform accelerates the gelation process. There is also evidence from IR which shows that the orientation of the ring plane is perpendicular to the chain axis. This suggests that there is a strong interaction between benzene and sPS molecules. The other interesting observation came from studies on decalin sPS and iPS systems. iPS forms a transparent gel and then becomes turbid, gradually forming trigonal crystallites of iPS. sPS does not convert to a gel but the fine crystalline precipitate particles instead. This shows that the molecular arrangement depends on both the solvent type and on the molecular structure of the polymer.[2]

Figure 12.1.30 shows how benzene molecules align themselves parallel to the phenyl rings of polystyrene and how they are housed within the helical form of the polymer structure which is stabilized by the presence of solvent.[1]

Work on poly(ethylene oxide) gels[7] indicates that the presence of solvents such as chloroform and carbon disulfide contributes to the formation of a uniform helical conformation. The gelation behavior and the gel structure depend on the solvent type which, in turn, is determined by solvent-polymer interaction. In a good solvent, polythiophene molecules exist in coiled conformation. In a poor solvent, the molecules form aggregates through the short substituents.[8]

Polyvinylchloride, PVC, which has a low crystallinity, gives strong gels. Neutron diffraction and scattering studies show that these strong gels result from the formation of

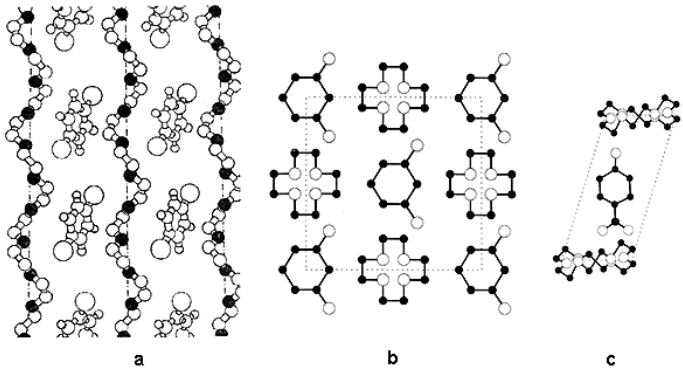

Figure 12.1.33. Crystal structure of poly(ethylene oxide) molecular complex with: (a) p-dichlorobenzene, (b) resorcinol, (c) p-nitrophenol. [Adapted, by permission, from M Dosiere, *Macromol. Symp*., **114**, 51 (1997).]

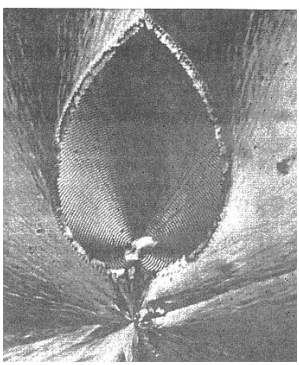

Figure 12.1.34. Optical micrograph of PEO-resorcinol complex. [Adapted, by permission, from M Dosiere, *Macromol. Symp*., **114**, 51 (1997).]

PVC-solvent complexes.[9] This indicates that the presence of solvent may affect the mechanical properties of such a system. Figure 12.1.31 shows that the presence of dichloromethane in sPS changes the mechanical characteristic of the material. A solvent-free polymer has a high elongation and yield value. An oriented polymer containing dichloromethane has lower elongation, no yield value, and approximately four times greater tensile strength.[10]

The interaction of polymer-solvent affects rheological properties. Studies on a divinyl ether-maleic anhydride copolymer show that molecular structure of the copolymer can be altered by the solvent selected for synthesis.[11] Studies have shown that the thermal and UV stability of PVC is affected by the presence of solvents.[12-14]

Figure 12.1.32 shows that solvent type and its molar fraction affect the value of the carbonyl frequency shift. This frequency shift occurs at a very low solvent concentration, The slope angles for each solvent are noticeably different.[15] Similar frequency shifts were reported for various solvents in polyetheretherketone, PEEK, solutions.[16]

These associations are precursors of further ordering by crystallization. Figure 12.1.33 shows different crystalline structures of poly(ethylene oxide) with various solvents.[17] Depending on the solvent type, a unit cell contains a variable number of monomers and molecules of solvent stacked along the crystallographic axis. In the case of dichlorobenzene, the molecular complex is orthorhombic with 10 monomers and 3 solvent molecules. Figure 12.1.34 shows optical micrograph of spherulite formed from unit cells having 8 monomers and 4 molecules of solvent. The unit cell of the triclinic crystal, formed with nitrophenol, is composed of 6 monomers and 4 molecules of solvent. This underlines the importance of solvent selection in achieving the desired structure in the formed material. The technique is also advantageous in polymer synthesis, in improving polymer stability, etc.

Temperature is an essential parameter in the crystallization process.[18] Rapid cooling of a polycarbonate, PC, solution in benzene resulted in extremely high crystallinity (46.4%) as compared to the typical PC crystallinity of about 30%.

Polymer-solvent interaction combined with the application of an external force leads to the surface crazing of materials. The process is based on similar principles as discussed in this section formation of fibrilar crystalline structures.

Although research on molecular structure and crystallization is yet to formulate a theoretical background which might predict the effect of different solvents on the fine structure of different polymers, studies have uncovered numerous issues which cause concern but which also point to new applications. A major concern is the effect of solvents on craze formation, and on thermal and UV degradation. Potential applications include engineering of polymer morphology by synthesis in the presence of selected solvent under a controlled thermal regime, polymer reinforcement by interaction with smaller molecules, better retention of additives, and modification of surface properties to change adhesion or to improve surface uniformity, etc.

REFERENCES

1 J M Guenet, *Macromol. Symp*., **114**, 97 (1997).
2 M Kobayashi, *Macromol. Symp*., **114**, 1-12 (1997).
3 T Nakaoki, M Kobayashi, *J. Mol. Struct*., **242**, 315 (1991).
4 M Kobayashi, T Nakoaki, *Macromolecules*, **23**, 78 (1990).
5 M Kobayashi, T. Kozasa, *Appl. Spectrosc*., **47**, 1417 (1993).
6 M. Kobayashi, T Yoshika, M Imai, Y Itoh, *Macromolecules,* **28**, 7376 (1995).
7 M Kobayashi, K Kitagawa, *Macromol. Symp*., **114**, 291 (1997).
8 P V Shibaev, K Schaumburg, T Bjornholm, K Norgaard, *Synthetic Metals*, **97**, No.2, 97-104 (1998).
9 H Reinecke, J M Guenet, C. Mijangos, *Macromol. Symp*., **114**, 309 (1997).
10 C Daniel, L Guadagno, V Vittoria, *Macromol. Symp.*, **114**, 217 (1997).
11 M Y Gorshkova, T L Lebedeva, L L Stotskaya, I Y Slonim, *Polym. Sci. Ser. A*, **38**, No.10, 1094-6 (1996).
12 G Wypych, **Handbook of Material Weathering**, *ChemTec Publishing*, Toronto, 1995.
13 G Wypych, **Poly(vinyl chloride) degradation**, *Elsevier*, Amsterdam, 1985.
14 G Wypych, **Poly(vinyl chloride) stabilization**, *Elsevier*, Amsterdam, 1986.
15 J M Gomez-Elvira, P Tiemblo, G Martinez, J Milan, *Macromol. Symp*., **114**, 151 (1997).
16 B H Stuart, D R Williams, *Polymer*, **36**, No.22, 4209-13 (1995).
17 M Dosiere, *Macromol. Symp*., **114**, 51 (1997).
18 Gending Ji, Fengting Li, Wei Zhu, Qingping Dai, Gi Xue, Xinhong Gu, *J. Macromol. Sci. A*, **A34**, No.2, 369-76 (1997).
19 I V Bykova, E A Sinevich, S N Chvalun, N F Bakeev, *Polym. Sci. Ser. A*, **39**, No.1, 105-12 (1997).

12.1.5 OTHER PROPERTIES AFFECTED BY SOLVENTS

Many other properties of solutes and solutions are affected by solvents. Here, we will discuss material stability and stabilization, some aspects of reactivity (more information on this subject appears in Chapter 13), physical properties, some aspects of electrical and electrochemical properties (more information on this subject appears in Chapter 11), surface properties, and polarity and donor properties of solvents.

Degradative processes have long been known to be promoted by the products of solvent degradation. Tetrahydrofuran is oxidized to form a peroxide which then dissociates to form two radicals initiating a chain of photo-oxidation reactions. Figure 12.1.35 shows the kinetics of hydroperoxide formation.[1] Similar observations, but in polymer system, were made in xylene by direct determination of the radicals formed using ESR.[2] An increased concentration in trace quantities of xylene contributed to the formation of n-octane radicals

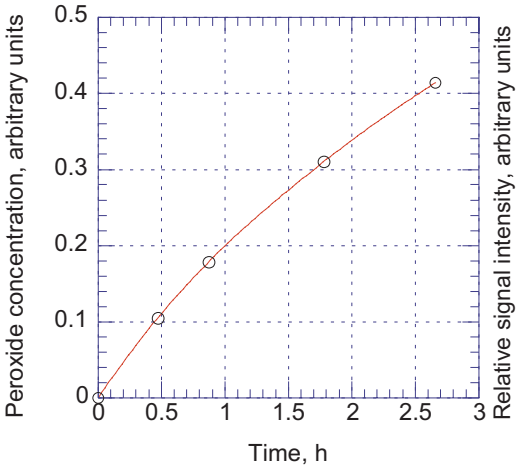

Figure 12.1.35. Peroxide formation from tetrahydrofuran during irradiation at 254 nm. [Data from J F Rabek, T A Skowronski, B Ranby, *Polymer*, **21**, 226 (1980).]

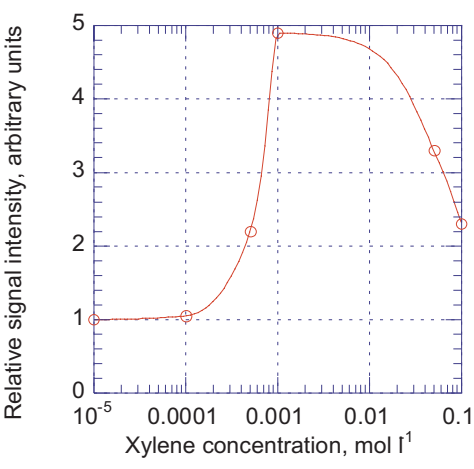

Figure 12.1.36. Spectral intensity of n-octane radical formed during irradiation of PE at -196°C for 30 min vs. concentration of p-xylene. [Adapted, by permission, from H Kubota, M Kimura, *Polym. Deg. Stab.*, **38**, 1 (1992).]

by abstracting hydrogen from polyethylene chain in an α-position to the double bond (Figure 12.1.36).

3-hydroperoxyhexane cleaves with formation of carboxylic acid and hydrocarbon radical (ethylene or propylene).[3] These known examples show that the presence of even traces of solvents may change the chemistry and the rate of photo-oxidative processes because of formation of radicals.

In another aspect of photo-oxidative processes, solvents influence the reactivity of small molecules and chain segments by facilitating the mobility of molecules and changing the absorption of light, the wavelength of emitted fluorescent radiation, and the lifetime of radicals. Work on anthraquinone derivatives, which are common photosensitizers, has shown that when photosensitizer is dissolved in isopropanol (hydrogen-donating solvent) the half-life of radicals is increased by a factor of seven compared to acetonitrile (a non-hydrogen-donating solvent).[4] This shows that the ability of a photosensitizer to act in this manner depends on the presence of a hydrogen donor (frequently the solvent). In studies on another group of photosensitizers – 1,2-diketones, the solvent cyclohexane increased the absorption wavelength of the sensitizer in the UV range by more than 10 nm compared with solutions in ethanol and chloroform.[5] Such a change in absorption may benefit some systems because the energy of absorbed radiation will become lower than the energy required to disrupt existing chemical bonds. But it may also increase the potential for degradation by shifting radiation wavelength to the range absorbed by a particular material. Presence of water may have a plasticizing action which increases the mobility of chains and their potential for interactions and reactions.[6]

Studies on photoresists, based on methacryloyethyl- phenylglyoxylate, show that, in aprotic solvents, the main reaction mechanism is a Norrish type II photolysis leading to chain scission.[7] In aprotic solvents, the polymer is photoreduced and crosslinks are formed.

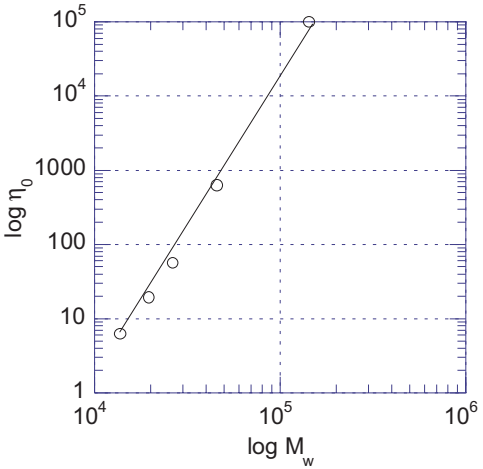

Figure 12.1.37. Effect of viscosity on molecular weight of polyethylene wax obtained by thermolysis in the presence of phenylether at 370°C. [Adapted, by permission, from L Guy, B Fixari, *Polymer*, **40**, No.10, 2845-57 (1999).]

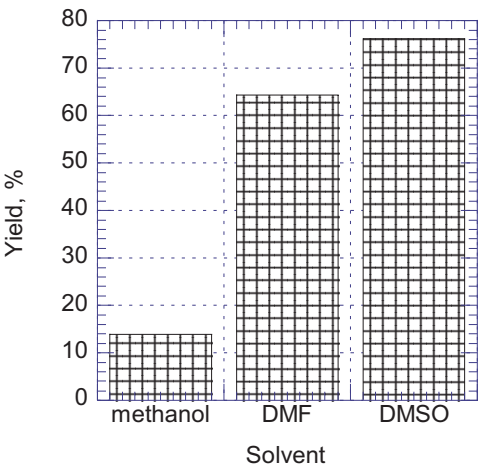

Figure 12.1.38. Yield of condensation products depending on solvent. [Adapted, by permission, from J Jeczalik, *J. Polym. Sci.: Polym. Chem. Ed.,* **34**, No.6, 1083-5 (1996).]

Polarity of the solvent determines quantum yields in polyimides.[8] The most efficient photocleavage was in medium-polar solvents. The selection of solvent may change the chemical mechanism of degradation and the associated products of such reactions.

Singlet oxygen is known to affect material stability by its ability to react directly with hydrocarbon chains to form peroxides. The photosensitizers discussed above are capable of generating singlet oxygen. Solvents, in addition to their ability to promote photosensitizer action, affect the lifetime of singlet oxygen (the time it has to react with molecules and form peroxides). Singlet oxygen has very short lifetime in water (2 μs) but much longer times in various solvents (e.g., 24 μs in benzene, 200 μs in carbon disulfide, and 700 μs in carbon tetrachloride).[9] Solvents also increase the oxygen diffusion coefficient in a polymer. It was calculated[10] that in solid polystyrene only less than 2% of singlet oxygen is quenched compared with more than 50% in solution. Also, the quantum yield of singlet oxygen was only 0.56 in polystyrene and 0.83 in its benzene solution.[10]

The photostabilizer must be durable. It was found that salicylic stabilizers are efficiently degraded by singlet oxygen in polar alkaline media but in a less polar, non-alkaline solvents these stabilizers are durable.[11] In hydrogen-bonding solvents, the absorption spectrum of UV absorbers is changed.[12]

Thermal decomposition yield and composition of polystyrene wastes is affected by addition of solvents.[13] Solvents play two roles: First, they stabilize radicals and, second, by lowering solution viscosity they contribute to homogeneity, increase the mobility of components and increase reactivity. 85% benzyl and phenoxy radicals were stabilized by hydrogens from tetralin.[13] In polyethylene thermolysis, the use of solvent to reduce viscosity resulted in obtaining lower molecular weight, narrow molecular weight distribution and high crystallinity in resultant polyethylene wax.[14] Figure 12.1.37 illustrates the relationship

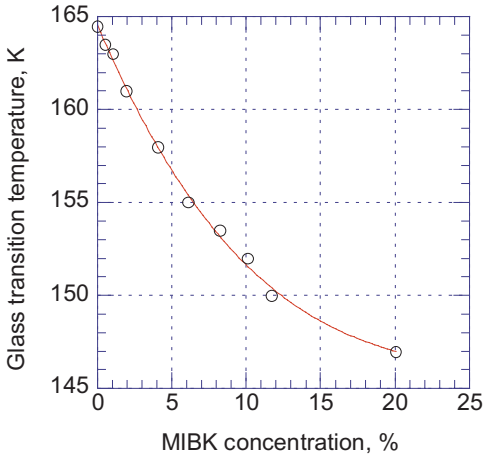

Figure 12.1.39. Glass transition temperature of perfluoro polyoxyalkylene oligomers vs. MIBK concentration. [Data from S Turri, M Scicchitano, G Gianotti, C Tonelli, *Eur. Polym. J.*, **31**, No.12, 1227-33 (1995).]

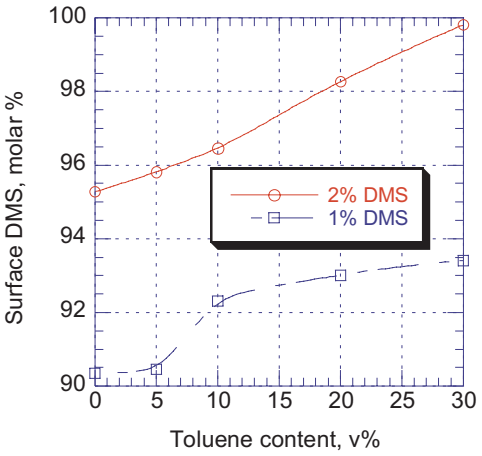

Figure 12.11.40. Surface DMS vs. toluene concentration for two bulk contents of DMS in polystyrene. [Data from Jiaxing Chen, J A Gardella, *Macromolecules*, **31**, No.26, 9328-36 (1998).]

between molecular weight and viscosity of solutions of polyethylene in phenylether as a solvent.[14]

Figure 12.1.38 shows that polymerization yield depends on the solvent selected for the polymerization reaction. The polymerization yield increases as solvent polarity increases.[15] Work on copolymerization of methyl methacrylate and N-vinylpyrrolidone shows that the solvent selected regulates the composition of copolymer.[16] The smaller the polarity of the solvent and the lower the difference between the resonance factors of the two monomers the more readily they can copolymerize. Work on electropolymerization[17] has shown an extreme case of solvent effect in the electrografting of polymer on metal. If the donocity of the monomer is too high compared with that of the solvent, no electrografting occurs. If the donocities are low, a high dielectric constant of solvent decreases grafting efficiency. This work, which may be very important in corrosion protection, illustrates that a variety of influences may affect the polymerization reaction.

The addition of solvent to polymer has a plasticizing effect. The increase in free volume has a further influence on the glass transition temperature of the polymer. Figure 12.1.39 shows the effect of methyl-isobutyl-ketone, MIBK, at various concentrations on glass transition temperature.[18] Several solvents were used in this study[18] to determine if the additivity rule can be useful to predict the glass transition temperature of a polymer-solvent system. The results, as a rule, depart from the linear relationship between glass transition temperature and solvent concentration. Generally, the better the solvent is for a particular polymer the higher is the departure.

Hydrogen bond formation as a result of the interaction of polymer with solvent was found to contribute to changes in the electric properties of polyaniline.[19] Hydrogen bonding causes changes in conformal structure of polymer chains. This increases the electrical conductivity of polyaniline. Water is especially effective in causing such changes but other hy-

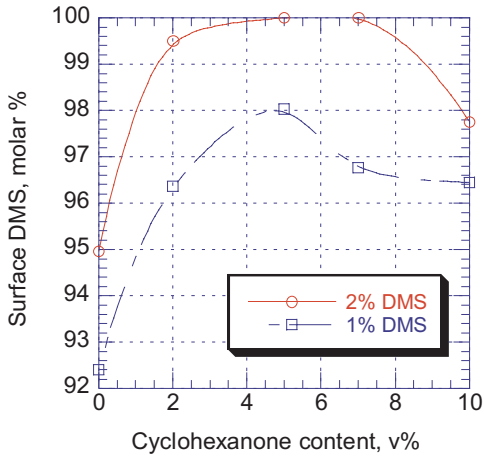

Figure 12.1.41. Surface DMS vs. cyclohexanone concentration for two bulk contents of DMS in polystyrene. [Data from Jiaxing Chen, J A Gardella, *Macromolecules*, **31**, No.26, 9328-36 (1998).]

drogen bonding solvents also affect conductivity.[19] This phenomenon is applied in antistatic compounds which require a certain concentration of water to perform their function.

Surface properties such as smoothness and gloss are affected by the rheological properties of coatings and solvents play an essential role in these formulations. Surface composition may also be affected by solvent. In some technological processes, the surface composition is modified by small additions of polydimethylsiloxane, PDMS, or its copolymers. The most well known application of such technology has been the protection of external surface of the space shuttle against degradation using PDMS as the durable polymer. Other applications use PDMS to lower the coefficient of friction . In both cases, it is important that PDMS forms a very high concentrations on the surface (possibly 100%). Because of its low surface energy, it has the intrinsic tendency to migrate to the surface consequently, surface concentrations as high as 90% can be obtained without special effort. It is more difficult to further increase this surface concentration. Figure 12.1.40 shows the effect of a chloroform/toluene mixture on the surface segregation of PDMS. When the poor solvent for PDMS (toluene) is mixed with chloroform, the decrease in the mobility of the PDMS segments makes the cohesive migration of the polystyrene, PS, segments more efficient and the concentration of PDMS on the surface increases as the concentration of toluene increases. Increase in PDMS concentration further improves its concentration on the surface to almost 100%. This shows the influence of polymer-solvent interaction on surface segregation and demonstrates a method of increasing the additive polymer concentration on the surface. Solvents with higher boiling points also increase surface concentration of PDMS because they extend the time of the segregation process.[20]

Figure 12.1.41 shows the effect of addition of cyclohexanone to chloroform.[20] This exemplifies yet another phenomenon which can help to increase the surface concentration of PDMS. Cyclohexanone is more polar solvent than chloroform (Hansen parameter, δ_p, is 3.1 for chloroform and 6.3 for cyclohexanone). The solvation of cyclohexanone molecules will selectively occur around PDMS segments which helps in the segregation of PDMS and in the cohesive migration of PS. But the figure shows that PDMS concentration initially increases then decreases with further additions of cyclohexanone. The explanation for this behavior is in the amount of cyclohexanone required to better solvate PDMS segments. When cyclohexanone is in excess, it also increases the solvation of PS and the effect which produces an increased surface segregation is gradually lost.

The surface smoothness of materials is important in solvent welding. It was determined that a smooth surface on both mating components substantially increases the strength of the weld.[21] This finding may not be surprising since weld strength depends on close sur-

face contact but it is interesting to note that the submicrostructure may have an influence on phenomena normally considered to be influenced by features which have a larger dimensional scale. Non-blistering primer is another example of a modification which tailors surface properties.[22] The combination of resins and solvents used in this invention allows solvent to escape through the surface of the cured primer before the material undergoes transitions that occur at high temperatures. Additional information on this subject can be found in Chapter 7.

A review paper[23] examines the nucleophilic properties of solvents. It is based on accumulated data derived from calorimetric measurements, equilibrium constants, Gibbs free energy, nuclear magnetic resonance, and vibrational and electronic spectra. Parameters characterizing Lewis-donor properties are critically evaluated and tabulated for a large number of solvents. The explanation of the physical meaning of polarity and discussion of solvatochromic dyes as the empirical indicators of solvent polarity are discussed (see more on this subject in Chapter 10).[23]

REFERENCES

1 J F Rabek, T A Skowronski, B Ranby, *Polymer*, **21**, 226 (1980).
2 H Kubota, M Kimura, *Polym. Deg. Stab*., **38**, 1 (1992).
3 G Teissedre, J F Pilichowski, J Lacoste, *Polym. Degrad. Stability*, **45**, No.1, 145-53 (1994).
4 M Shah, N S Allen, M Edge, S Navaratnam, F Catalina, *J. Appl. Polym. Sci*., **62**, No.2, 319-40 (1996).
5 P Hrdlovic, I Lukac, *Polym. Degrad. Stability*, **43**, No.2, 195-201 (1994).
6 M L Jackson, B J Love, S R Hebner, *J. Mater. Sci. Materials in Electronics*, **10**, No.1, 71-9 (1999).
7 Hu Shengkui, A Mejiritski, D C Neckers, *Chem. Mater*., **9**, No.12, 3171-5 (1997).
8 H Ohkita, A Tsuchida, M Yamamoto, J A Moore, D R Gamble, *Macromol. Chem. Phys*., **197**, No.8, 2493-9 (1996).
9 G Wypych, **Handbook of Material Weathering**, *ChemTec Publishing*, Toronto, 1995.
10 R D Scurlock, D O Martire, P R Ogilby, V L Taylor, R L Clough, *Macromolecules*, **27**, No.17, 4787-94 (1994).
11 A T Soltermann, D de la Pena, S Nonell, F Amat-Guerri, N A Garcia, *Polym. Degrad. Stability*, **49**, No.3, 371-8 (1995).
12 K P Ghiggino, *J. Macromol. Sci. A*, **33**, No.10, 1541-53 (1996).
13 M Swistek, G Nguyen, D Nicole, *J. Appl. Polym. Sci*., **60**, No.10, 1637-44 (1996).
14 L Guy, B Fixari, *Polymer*, **40**, No.10, 2845-57 (1999).
15 J Jeczalik, *J. Polym. Sci.: Polym. Chem. Ed.,* **34**, No.6, 1083-5 (1996).
16 W K Czerwinski, *Macromolecules*, **28**, No.16, 5411-8 (1995).
17 N Baute, C Calberg, P Dubois, C Jerome, R Jerome, L Martinot, M Mertens, P Teyssie, *Macromol. Symp*., **134**, 157-66 (1998).
18 S Turri, M Scicchitano, G Gianotti, C Tonelli, *Eur. Polym. J*., **31**, No.12, 1227-33 (1995).
19 E S Matveeva, *Synthetic Metals*, **79**, No.2, 127-39 (1996).
20 Jiaxing Chen, J A Gardella, *Macromolecules*, **31**, No.26, 9328-36 (1998).
21 F Beaume, N Brown, *J. Adhesion*, **47**, No.4, 217-30 (1994).
22 M T Keck, R J Lewarchik, J C Allman, **US Patent 5,688,598**, Morton International, Inc., 1996.
23 Ch Reichardt, *Chimia*, **45**(10), 322-4 (1991).

12.2 CHAIN CONFORMATIONS OF POLYSACCHARIDES IN DIFFERENT SOLVENTS

Ranieri Urbani and Attilio Cesàro
Department of Biochemistry, Biophysics and Macromolecular Chemistry, University of Trieste, Italy

12.2.1 INTRODUCTION

Carbohydrate monomers and polymers are present in all living organisms and are widely used in industrial applications. In life forms they show and express very diverse biological functions: as structural, storage and energy materials, as specific molecules in the immunochemistry of blood, as important polymers of cell walls determining cell-cell recognition,[1] antigenicity and viral infection, etc..

The variability of primary structure and conformation makes the carbohydrate molecule extremely versatile, for example, for specific recognition signals on the cell surface.[2] In any biological system whatsoever the shape and size adopted by carbohydrates in different solvent environments have been widely demonstrated to be responsible for the biological function of these molecules.

In recent years, significant progress has been made in the improvement of both the experimental and theoretical research tools needed to study the conformational complexity of carbohydrates in solution, such as X-ray and neutron scattering techniques (SAXS and SANS), atomic force microscopy (AFM), high-resolution NMR spectroscopy and relaxation techniques, and computational methods. All the experimental and computational methods unequivocally indicate the relevance of the environment (e.g., solvent composition, pH and salt conditions, temperature) on the topological shape and the properties of the carbohydrate solutes. The general problem of solvent effect on the conformational states and the preferential solvation of oligo- and polysaccharides has been tackled mainly to validate detailed molecular models which were developed for relating the structural characteristics of these macromolecules to their chemical, physical, and biological properties in solution.[3-5] Semi-empirical methods (unrefined in the sense that molecular parameters are not adjusted for the specific case studied) have been proven useful and generally applicable to different chain linkages and monomer composition. However, it must be clear that all these methods, unless specifically stated otherwise, refer to calculations of the unperturbed chain dimension and therefore do not take into account the excluded volume effects (which arise typically from long-range interactions). In most cases, solvation effects (which are short range) are not explicitly taken into consideration, e.g., molecular parameters of the solvent do not enter in the calculations, although some exceptions are found in literature.

The rationale for the correct setting of current knowledge about the shape of polysaccharides in solution is based on three factors: the correlation between primary structure (i.e., the chemical identity of the carbohydrates polymerized in the chain), intrinsic conformational features dictated by the rotational equilibria (often the major contributions are due to the rotation about the glycosidic linkages) and the interaction with the other mo-

lecular species in the system (mainly the solvent which determines, therefore, the solubility of the chains).

In this chapter the description of the solvent effect is given within the framework of some specific experimental results and computational methods for studying and predicting oligo- and polysaccharide conformations in solution. It is not the authors' intention to make an in depth investigation into the general methodologies which have been widely reported over recent years (and in this book) but rather to provide a step-wise presentation of some conformational features which have upheld theoretical predictions with experimental observations. The number of examples and approaches is necessarily limited and the choice undoubtedly reflects the authors' preferences. Nonetheless, the aim is to be as informative as possible about the conceptual difficulties and conceivable results.

12.2.2 STRUCTURE AND CONFORMATION OF POLYSACCHARIDES IN SOLUTION

12.2.2.1 Chemical structure

The primary structure of polysaccharides (glycans) is often complicated by different kinds of linkages in homopolymers and different kinds of monomeric units, which give rise to a huge number of different polymers. Glucans (see a general formula in Figure 12.2.1) are those composed exclusively of glucose, while glucuronans are polymers of glucuronic acid. Similarly mannans and galactans as well as mannuronans and galacturonans, are homopolymers of mannose, galactose, mannuronic acid and galacturonic acid, respectively. Although all the polysaccharides discussed here show a structural regularity, they may not be simple homopolymers. Their chemical structure can sometimes be fairly complicated.

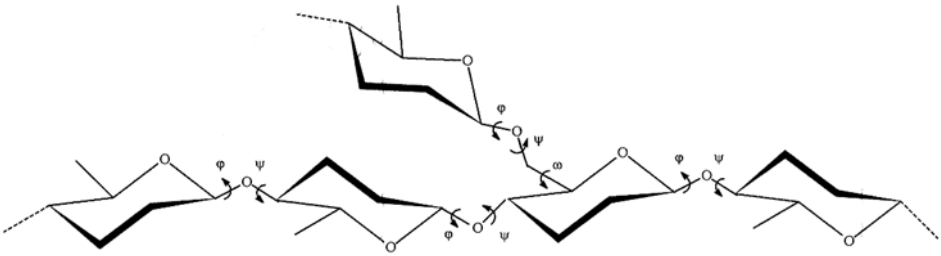

Figure 12.2.1. Example of the chemical structure of a polysaccharidic chain as a sequence of β-(1-4)- linked D-glucose units having a side chain of β-glucose linked (1-6) to the backbone. The glycosidic dihedral angles are also indicated.

12.2.2.2 Solution chain conformation

A regularity of primary structure could imply that the chains may assume ordered helical conformations, either of single or multiple strand type, both in the solid state and in solution. A knowledge of both polysaccharidic chain structure, up to the three-dimensional molecular shape, and the interaction of the polymers with other molecular components, is essential, in order to understand their capability to form supramolecular structures, including physical gels, with specific rheological properties, which have important implications for controlling and upgrading properties in industrial applications. The rationale is that the physico-chemi-

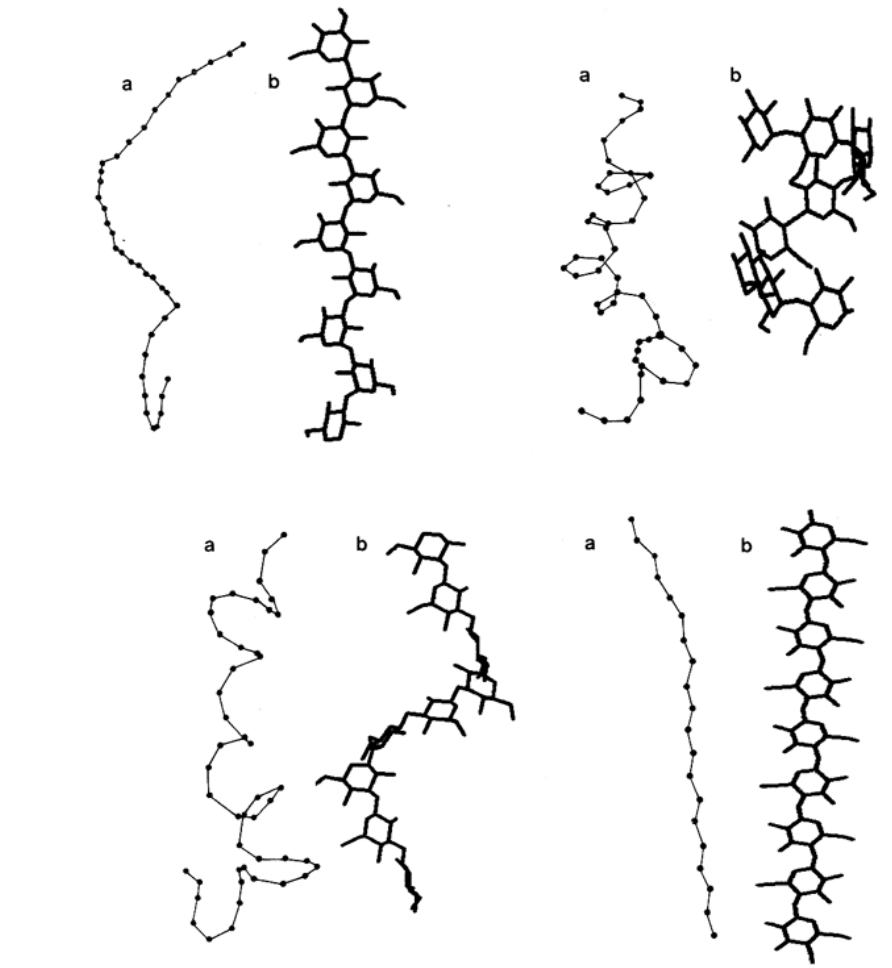

Figure 12.2.2. (a) Snapshot of random chains of homoglucans obtained from Monte Carlo calculation and (b) ordered helical structures of the same polymers as measured by X-ray diffraction method.

cal properties, which form the basis of the industrial applications of polysaccharides are directly related to the structure/conformation of the chain.

Many biological macromolecules in the solid state assume regular helices, which can be represented by means of a few geometrical parameters and symmetry relations. These helical structures originate from the stereo regularity of backbone monomers and are easily described, conceptually simple, and therefore used (all too often) as an idealized model for all the actual shapes. Elements of helical regularity are essential in the description of the structure of nucleic acids and polypeptides. Some biopolymers, e.g., globular proteins, almost completely preserve their structural regularity in solution. Such globular structures are not known in polysaccharides. Nonetheless, helical conformations have been proposed to represent the structure of many polysaccharides, microbial glycans in particular. An excellent overview of the stereo-regular helical conformations of polysaccharides deduced from X-ray fiber diffraction studies has recently been published.[6]

However, thermodynamic arguments suggest that a partially disordered state is an essential prerequisite for the stability of polymeric systems in solution. Under these circumstances, realistic chain pictures of polysaccharides will not necessarily be generated from the repetition of a single conformational state, which is usually identified by the minimum energy state found in the internal conformational energy calculations. Statistical approaches to these conformational energy surfaces[7,8] suggest a more disordered solution conformation (Figure 12.2.2, snapshots marked with a) than the chain structures proposed so as to fit the helical regularity deduced from x-ray fiber diffraction studies (Figure 12.2.2, structures marked with b). Thermal fluctuations are in general sufficient to generate delocalized disorder, unless diffuse interactions, cooperative in nature, ensure long-range order.

From the experimental point of view, several polysaccharides with different chain linkage and anomeric configuration have been studied to determine to what extent the polymeric linkage structure and the nature of the monomeric unit are responsible for the preferred solvation and for the chain topology and dimensions.[9] Conversely, since it is generally understood that the structure and topology of many macromolecules are affected by solvation, theoretical models must include these solvent effects in addition to the internal flexibility, in order to estimate changes in the accessible conformations as a result of the presence of the solvent molecules.

The concept of chain conformational disordering and dynamics in solution is associated with the existence of a multiplicity of different conformations with accessible energy and, moreover, exhibiting their topological differentiation. The above conformational variability of polymeric chains is implicitly recognizable by the great difficulty in crystallization and by the typical phenomenon of polymorphism. This discussion is relevant in particular to ionic polysaccharides (see below) because, from the polyelectrolytic point of view, the transition from a more compact conformation (also an "ordered chain") to an extended coil conformation, is usually associated with a net variation in ionic charge density along the chain.

Polysaccharides generally dissolve only in strongly solvating media. Water displays a complicated behavior: it is a good solvent for monomers and oligosaccharides inasmuch as it is able to compete with the specific inter- and intra-molecular hydrogen bond network (Figure 12.2.3). In many cases it is the thermodynamic stability of the solid-state form which protects the solute molecules from being solubilized.[10] Nevertheless, some other strong solvents, such as, dimethylsulfoxide, DMSO, and 1,4-dioxane are known to be good solvents for carbohydrate polymers. Many commercial applications of polysaccharides require compatibility with different solvents and solutes (organic solvents, salts, emulsifiers, plasticizers, enzymes, etc.), for example, in pharmaceutical matrices, paints and foods. In this field, solvent compatibility of some glycans has been improved and controlled by functionalization and derivatization in order to obtain a proper degree of substitution, which determines a wide range of compatibility properties.

At the molecular level, various specific and non-specific solvent-solute interactions may occur in polysaccharide solutions that may result in a change in the conformational shape, solubility, viscosity and other hydrodynamic and thermodynamic properties. Hydrophilic interactions such as hydrogen bonding and electrostatic interactions are believed to be factors that influence the conformation of polysaccharides in solution, although the question is being raised (more and more) as to the implication of patches of hydrophobic intermolecular interactions, especially for chain aggregations. One important feature is the

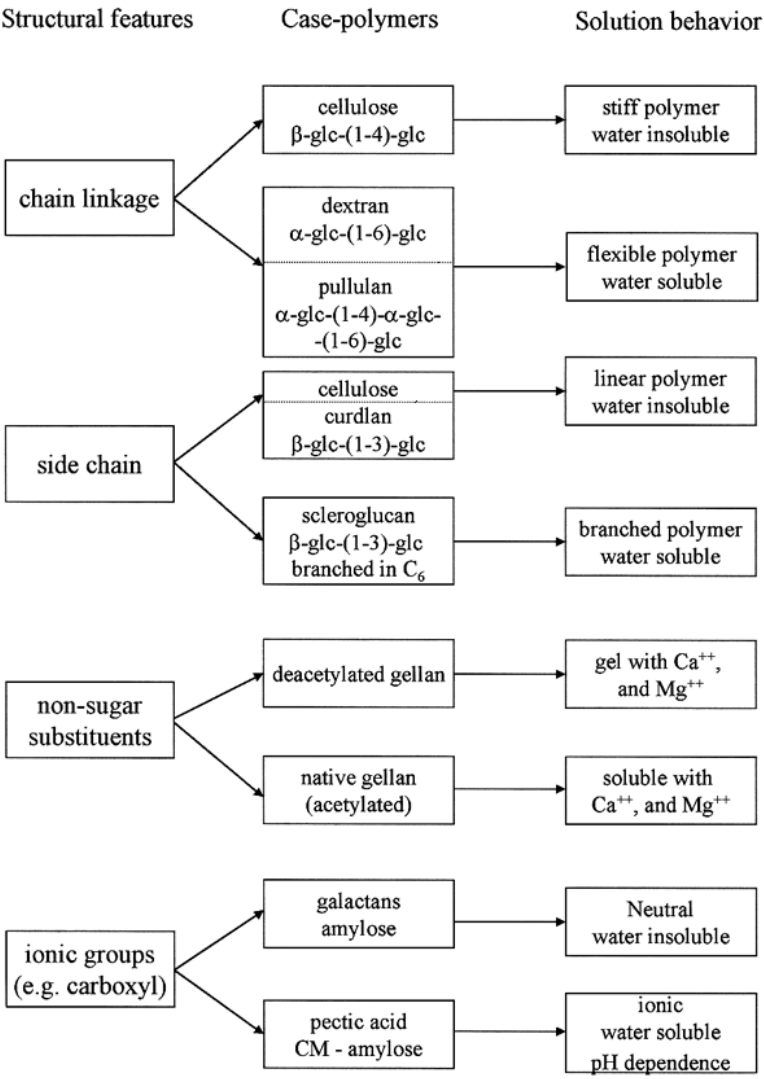

Figure 12.2.3. Role of structural, conformational and substituent features on the solution properties of oligo- and polysaccharides.

surface that saccharide segments address to solvent molecules that allows a high degree of favorable interactions. The water structuring in the solvation of polysaccharides also contributes to the stability of saccharides in solution,[11] which may be altered by competition of other co-solutes or co-solvents which are able to modify the extent of hydrogen-bonded interactions among components. Urea, for example, is considered a breaker of ordered polysaccharide conformation in gel networks, such as those obtained with agar and carrageenan as well as with microbial polysaccharides.

Over the last twenty years or so, several approaches have been made to determine the three-dimensional structure of oligosaccharides and theoretical calculations are becoming

an increasingly important tool for understanding the structure and solution behavior of saccharides.[11-15] Although computer facilities and calculation speeds have grown exponentially over the years some of these techniques, like quantum mechanic methods (ab initio methods), have been shown not to be useful in dealing with the complexity of systems which involve many atoms such as in macromolecular systems. On the other hand, these techniques have been successfully applied to small molecules, e.g., mono- and disaccharides, in predicting charge distribution on the atoms, conformations and transitions among accessible conformations,[16] thus providing a background knowledge for the more complicated systems.

12.2.3 EXPERIMENTAL EVIDENCE OF SOLVENT EFFECT ON OLIGOSACCHARIDE CONFORMATIONAL EQUILIBRIA

The problem of sugar conformation and dynamics in solution is related to the question of to what extent are oligo- and polysaccharides intrinsically flexible under the different experimental conditions. The answer to this question, which requires a complete knowledge of the time-space dependence of the chain topology,[17] is often "rounded-off" by the use of empirical terms like "flexibility". A further problem is to what extent does the solvent contribute to stabilizing some conformational states rather than others. Solution properties are functions of the distribution of conformations of the molecules in the solvated states, in the sense that the experimental data are statistical thermodynamic averages of the properties over all the accessible conformational states of the molecule, taking each state with a proper statistical weight. This aspect can be better illustrated by taking into consideration the accessible conformational states of a simple sugar unit and the conformational perturbation arising from the changes in the interactions with the surrounding solvent medium.

For an α-pyranose ring, for example, the rotation about carbon-carbon bonds and the fluctuations of all ring torsional angles give rise to a great number of possible conformers with different energies (or probabilities). Some of these are identified as the preferred rotational isomeric states in various environments. The boat and boat-skew conformers of a pyranose ring, which are higher in energy than the preferred chair form, correspond to a major departure from the lowest energy chair conformation as illustrated by the globular conformational surface of Figure 12.2.4. Additional conformational mobility in a monosaccharide is due to the rotations of exocyclic groups, namely, OH and especially CH_2OH. Let us point out that in a polymer these ring deformations do not normally occur, but, when they do, they may determine to a great extent the equilibrium mean properties and the overall mean chain dimensions.[18,19] However, one very recent theory is that the elastic properties of amorphous polysaccharides are related to the glycosidic ring deformation.[20]

D-ribose is probably the best example of sugar that reaches a complex conformational equilibrium, giving rise to the mixture composition shown in Figure 12.2.5. The percentage of each form is taken from Angyal's data[21,22] with integration of the sub-splitting between the $^4C_1$ and the $^1C_4$ forms. The prime purpose of this analysis is to point out that the stability of each conformer is not determined solely by the intrinsic internal energy, which can be evaluated by means of e.g., ab-initio quantum mechanics calculations, but is strongly influenced by all the solvation contributions. Therefore, the conformer population may be shifted by changing temperature, solvent composition, or any other external variable such as, for example, adding divalent cations (see Table 12.2.1). The evaluation of the actual concentration of the several conformers involved in the equilibrium immediately leads to

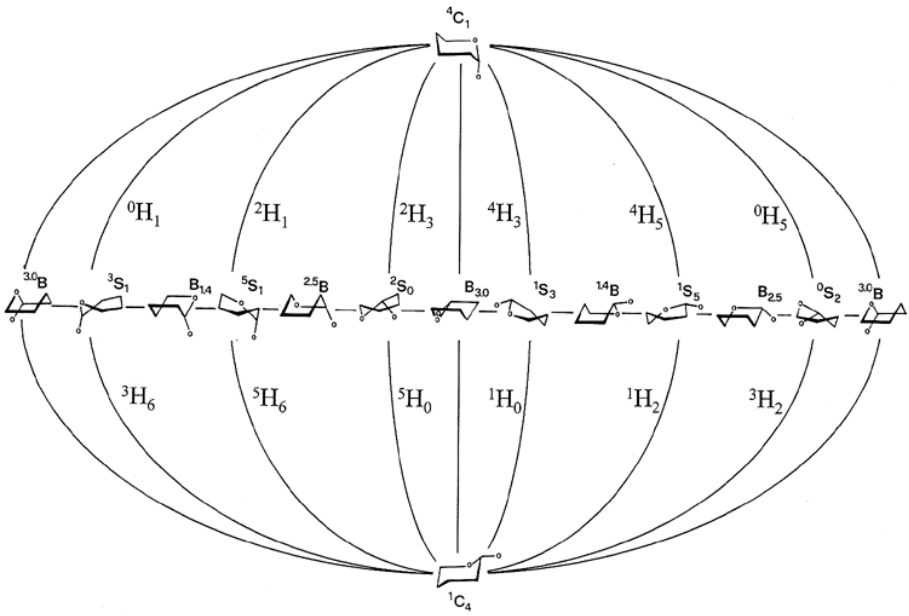

Figure 12.2.4. Representation of all possible conformations of the pyranosidic ring and respective inter-conversion paths.

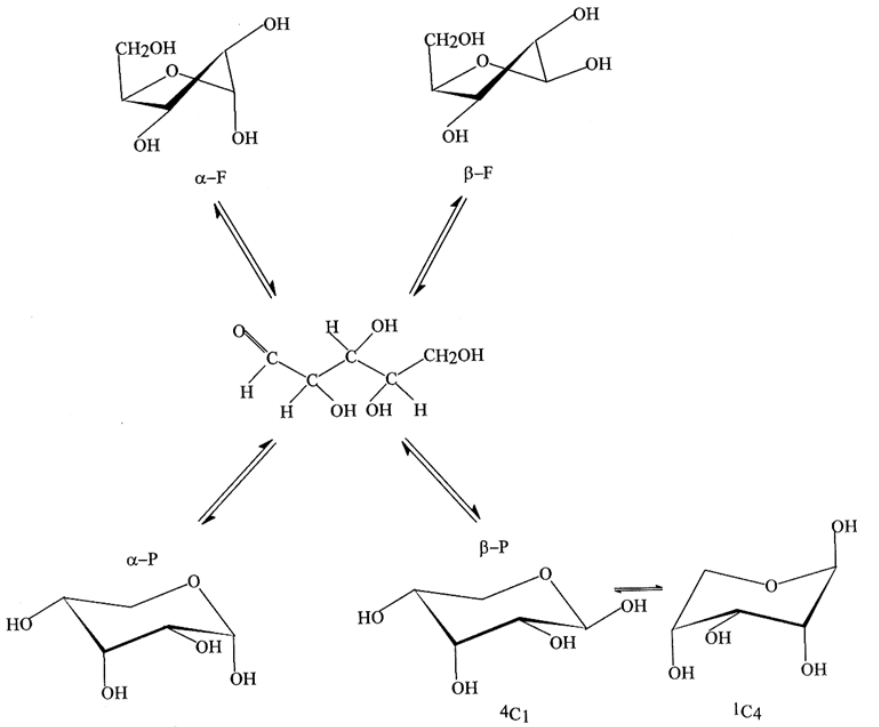

Figure 12.2.5. D-ribose conformational equilibria.

the partition function of the system (i.e., the free-energy change or the equilibrium constant for a transition between conformers).

Table 12.2.1. Percentage composition of furanose and pyranose forms of D-ribose and glucose in different solvent systems

Sugar	Solvent	α-F	β-F	α-P	($^4C_1$) β-P	($^1C_4$) β-P
D-ribose	H_2O, 31°C	13.5	6.5	21.5	44.0	14.5
	D_2O, 30°C	8.0	14.0	23.0	41.0	14.0
	DMSO, 30°C	6.0	22.0	16.2	31.0	24.8
	Ca^{2+}, 1.27 M	13.0	5.0	40.0	14.0	28.0
Glucose	DMSO, 17°C			45.0	55.0	
	pyridine, 25°C	0.6	1.0	45.0	53.0	

Passing from monomer units to oligomers (disaccharides and higher oligosaccharides), the dominant features of molecular flexibility become those due to rotations about the glycosidic linkages. Although other conformational fluctuations may contribute to the local dynamics of the atoms or group of atoms, only the glycosidic linkage rotations are able to dramatically change the conformational topology of oligomers at ambient temperature. The aim of a conformational analysis of oligosaccharides is thus to evaluate the probability (that is the energy) of all mutual orientations of the two monosaccharidic units, as a function of rotations about the glycosidic linkages, defined by the dihedral angles:

φ = [H1-C1-O1-Cm]

ψ = [C1-O1-Cm-Hm]

where m is the aglycon carbon number in the reducing ring. The important region of φ and ψ rotations is the one with energy variations in the order of kT, the thermal motion energy, because this may produce a large ensemble of accessible conformational states for the oligosaccharide. Even when the rotational motion is restricted to only a few angles, the fluctuations of many such glycosidic bonds is amplified along the chain backbone, as the molecular weight increases. The accumulation of even limited local rotations may produce very large topological variations in the case of polymeric chains and consequently relevant changes in thermodynamic, hydrodynamic and rheological properties of these systems. Other internal motions often make only small contributions to the observable properties on the macromolecular scale.[23]

Experimentally, NMR techniques are among the most valuable tools for studying conformations and dynamics of oligosaccharides in solution by determining chemical shifts, coupling constants, NOE's and relaxation time.[24-30] In the study of saccharide conformations the potential of coupling constants evaluation, specially the (hetero-nuclear) carbon-proton spin-spin coupling constants, $^nJ_{C,H}$, and their dependence on solvent medium is well known. Several empirical correlations between $^1J_{C,H}$ and structural parameters like dihedral angles have been reported,[31] although the low natural abundance of the ^{13}C isotope often made the measurements technically difficult and ^{13}C enrichment was required for the generation of data of sufficient quality for the quantitative analysis. Nowadays, due to the progress of FT-NMR spectrometers, measurements of the three-bond (vicinal) carbon-pro-

ton coupling constant, $^3J_{C,H}$ have indeed been made possible on the natural-abundance ^{13}C spectra. Much endeavor has been invested in establishing a general Karplus-like relation for the angular dependence of $^nJ_{C,H}$, especially on the dihedral angles in the glycosidic region because the overall three-dimensional structure of oligo- and polysaccharides are related to the glycosidic features in terms of dihedral (rotational) angles.

From comparison of experimental data and theoretical results (using quantum-mechanical and semi-empirical methods) on model compounds,[32-34] the angular dependence of the coupling constants, $^nJ_{C,H}$, on the anomeric and aglycon torsional angles φ and ψ,[31,34] and on the dielectric constant of the solvent[35] can be written in a general form such as:

$$^1J_{C,H} = A_1 \cos 2\chi + A_2 \cos\chi + A_3 \sin 2\chi + A_4 \sin\chi + A_5 + A_6\varepsilon$$

$$^3J_{C,H} = B_1 \cos^2\chi + B_2 \cos\chi + B_3 \sin\chi + B_4 \sin 2\chi + B_5 \qquad [12.2.1]$$

where:

A_i, B_i	constants different for α and β anomers
χ	φ or ψ
ε	solvent dielectric constant

Experimental $^nJ_{C,H}$ values for conformationally rigid carbohydrate derivatives allow to calculate the constant values of A_i and B_i in equations [12.2.1]. The major practical use of these equations is their ability to estimate the glycosidic dihedral angles from experimental $^nJ_{C,H}$ data, in combination with other complementary results, for example, from NOESY,[36] X-ray and chiro-optical experiments. Since the experimental values are averaged over all the accessible conformational states in solution, they do not necessary reflect the property of only the most probable conformer[23] but they nevertheless include contributions of all the conformers, each one taken with its proper statistical weight. Thus, the quantitative interpretation of experimental data in terms of accessible conformational states of flexible molecules requires the additional theoretical evaluation of the energy of the molecule as a function of internal coordinates. Since the dependence of the observed coupling constants on the conformation is non-linear, it derives that:

$$\left\langle {}^nJ_{C,H}(\chi)\right\rangle \neq {}^nJ_{C,H}\left(\langle\chi\rangle\right)$$

Only for a linear dependence of $^nJ_{C,H}$ on χ, the equation could hold the equals sign. Because of the simultaneous dependence of the property on χ and on the complexity of potential energy function, $E(\chi)$, the ensemble average of $<^nJ_{C,H}>$, as well as of any property of interest, can be calculated only by taking into consideration the conformational energy surface.

Apart from NMR and the methods suitable for characterization of overall chain dimensions (which we will touch on below), there are not many simple experimental techniques that can be used to study sugar conformation and that are directly correlated to theoretical results based on calculated potential energy surfaces or force fields. An exception is given by chiro-optical techniques, which provide important (although empirical) structural information as optical rotation experiments have been shown to be very useful and informative in the study of saccharides in solution.[37,38] Literature gives the experimental evidence for the effects of the external conditions (solvent and temperature) on the optical rotation. The additivity methods, proposed in the Fifties by Whiffen[39] and Brewster,[40] were

extended by Rees and co-workers,[37,41] who derived expressions for the contribution to the optical activity of changes in conformational states of oligo- and polysaccharide chains. More recently, Stevens and co-workers[42,43] developed a computational model for optical activity and circular dichroism based on the Kirkwood theory in which the calculations of the lowest energy component of a molecular $\sigma-\sigma^*$ transition, which derives from the mutual interaction of all $\sigma-\sigma^*$ transitions on C-C, C-H and C-O bonds, are carried out. The calculated optical properties are therefore geometry-dependent and the optical properties have been calculated as statistically averaged properties over an ensemble of all possible conformations, theoretically obtained as a function of φ and ψ. This model also provides a useful tool for testing the quality of force field parametrizations and the possibility of some refinement of force constants for a non-explicit inclusion of solvent environment.

12.2.4 THEORETICAL EVALUATION OF SOLVENT EFFECT ON CONFORMATIONAL EQUILIBRIA OF SUGARS

12.2.4.1 Classical molecular mechanics methods

Theoretical approaches to the conformational analysis of oligosaccharides in solution become inherently more complicated than those for monomeric sugars, at least for the computer time required to optimize the structures. Depending on the degrees of freedom taken into consideration and on the level of sophistication of the method used, the conformational analysis may give different results. It has been the custom in the past to compute the conformational energy as a function of the dihedral angles φ and ψ only, by assuming the sugar ring to be rigid (rigid-residue method). More recently, all the internal coordinates are allowed to adjust at each increment of φ and ψ, relaxing the structure toward a local minimum (relaxed-residue method). The rigid-residue approach is still considered suitable as a starting point, although some warning must be alerted to the use of the same set of structural coordinates for all sugars, as was initially done. The approach may however be useful as a starting point in the conformational analysis of polysaccharides, provided that the coordinates of all the atoms in the monomeric unit have been calculated by a suitable independent method.[13, 44]

Figure 12.2.6 reports, as a general example, the rigid-residue energy surfaces of two representative disaccharides, namely α-(1-4)-D-glucopyranosil-D-glucopyranose (D-maltose, Figure 12.2.6a) and the β-(1-4)-D-glucopyranosil-D-glucopyranose (D-cellobiose, Figure 12.26b). Both maps present multiple minima separated by barriers that are only a few kilocalories high. For many disaccharides the barriers between minima can be very high and they are often overestimated in the rigid-residue approximation.

In general, the conformational energy map shows that only a limited portion of the total φ, ψ conformation space is actually accessible to the dissaccharide at room temperature. The dissaccharide is not frozen into its lowest energy conformation, nevertheless the steep walls of the allowed region of conformational energy may dramatically limit the multiplicity of thermally accessible conformational states.

One useful method, for taking into account the effect of solvent media upon the conformational properties of glycosidic structures, is the continuum reaction field method.[45, 46] This method is based on the Scaled Particle Theory (SPT) equations[47] and on Onsager's theory of the reaction field, as applied by Abraham[48] by considering the solvent as a dielectric continuum. In this approach the total conformational energy, G_{tot}, is given by:

$$G_{tot} = G_{conf} + G_{solv}$$

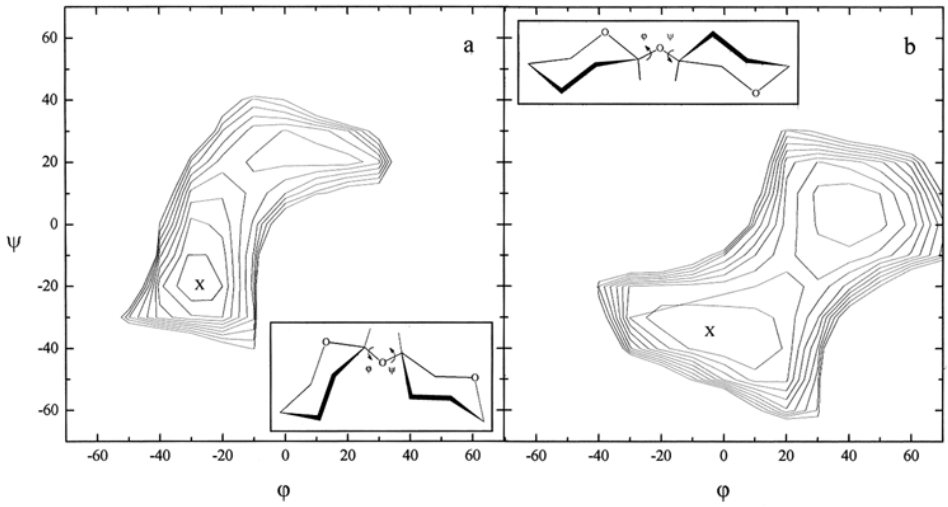

Figure 12.2.6. Conformational energy maps calculated for (a) D-maltose and (b) D-cellobiose. Contours are in kcal·mol^{-1} with increments above the minimum (x) of 0.5 kcal·mol^{-1}.

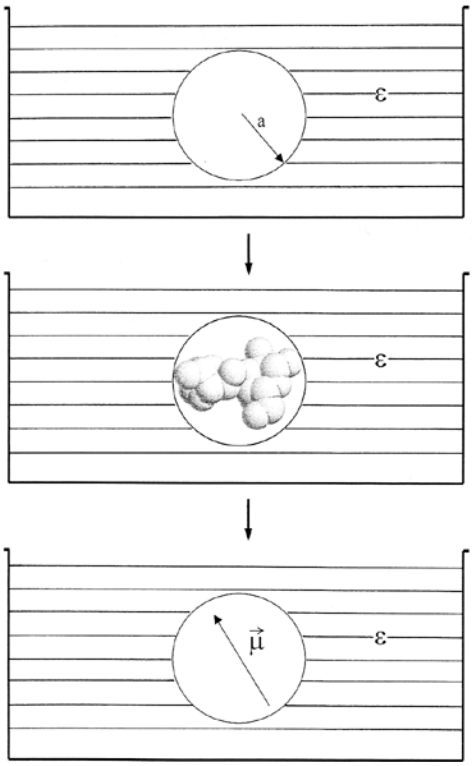

Figure 12.2.7. General scheme of the theoretical approach for the solvation energy calculation.

where the total conformational free energy, G_{tot}, is given by the sum of the contribution due to the in vacuo conformational state energy, G_{conf}, and the solvation contribution, G_{solv}. The latter term is a sum of contributions due to the energy required to create, in a given solvent, a cavity of suitable size to accommodate the solute molecule in a given conformational state and the interaction energy between the solute and the surrounding solvent molecules, as schematically shown in Figure 12.2.7:[49]

$$G_{solv} = G_{cav} + G_{el} + G_{disp} \quad [12.2.2]$$

The expression for G_{cav}, that is the free energy required for the formation of a cavity (first step in Figure 12.2.7), at a temperature T and a pressure P, is taken from the Scaled Particle Theory (SPT) which has been successfully applied in the study of thermodynamic properties of aqueous and non-aqueous solutions:[47,50]

$$\frac{G_{cav}}{RT} = -\ln(1-y) + \left(\frac{3y}{1-y}\right)\hat{R} + \left[\frac{3y}{1-y} + \frac{9}{2}\left(\frac{y}{1-y}\right)^2\right]\hat{R}^2 + \frac{yP}{\rho kT}\hat{R}^3 \quad [12.2.3]$$

where:

y	$= 4\pi\rho a_v^3 / 3$, the reduced number density
a_v, a_u	radii of hard sphere equivalent solute (u) and solvent (v) molecules
$\hat{R}$	$= a_u / a_v$
ρ	solvent density
R	gas constant
k	Boltzmann constant

It is noteworthy that G_{cav} is a function solely of solvent density and solvent and solute dimensions and represents a measure of the cohesive forces among solvent molecules. In a given solvent, this contribution is a function of the radius of solute molecule which may differ remarkably as a function of dihedral angles φ and ψ only.

The electrostatic interaction term G_{el} between solute and solvent is based on the continuum reaction field[48] which takes into account a reaction potential induced by the solute dipole and quadrupole (third step in Figure 12.2.7) in a continuum medium of dielectric constant ε:

$$G_{el} = \frac{KX}{1-IX} + \frac{3HX}{5-X}bF\left[1-\exp\left(-\frac{bF}{16RT}\right)\right] \quad [12.2.4]$$

with:

$$K = \frac{\mu_u^2}{a^3}, \quad H = \frac{Q_u^2}{a^5}, \quad I = \frac{2\left(n_u^2-1\right)}{n_u^2+2}, \quad X = \frac{\varepsilon-1}{2\varepsilon+1}$$

$$F = \begin{cases} 0 & for \quad \varepsilon \le 2 \\ \left[\dfrac{(\varepsilon-2)(\varepsilon+1)}{\varepsilon}\right]^{1/2} & for \quad \varepsilon > 2 \end{cases}$$

$$b = 4.35\left(\frac{T}{300}\right)^{1/2}\left(a^{3/2}r_{uv}^3\right)^3\left(\frac{K+Ha^2}{r_{uv}^2}\right)^{1/2}$$

where:

μ_u	solute dipole moment
Q_u	solute quadrupole moment
n_u	solute refractive index
a	$= a_v + a_u$
r_{uv}	$= a/2^{1/2}$

r_{uv} is the average distance between the solvent and the solute molecule defined in terms of the radius of cavity a.

The free energy of dispersion, G_{disp}, in equation [12.2.2] takes into account both attractive and repulsive non-bonding interactions and is expressed as a combination of the London dispersion equation and Born-type repulsion:[51]

$$G_{disp} = -0.327 N_v \alpha_u \alpha_v \frac{I_u I_v}{I_u + I_v} r_{uv}^{-6} \qquad [12.2.5]$$

where:

α	molecular polarizability
I	ionization potential
N_v	nearest-neighbor solvent molecules

N_v is the number of molecules surrounding the solute molecule in a given conformation and is calculated from the following equation:[52]

$$N_V = \left[\left(a_u + 2a_v \right)^3 - a_u^3 \right] \left(\frac{4\pi N_A}{3V_v} \right)^3$$

where:

V_v	solvent molar volume
N_A	Avogadro number

In order to elucidate the effect of different solvents on the conformation, the energy differences between conformers in a given solvent are more relevant than the absolute solvation energies in each solvent. In particular, it is important that the perturbation effect on the detailed shape in the low energy regions of the conformational map. Figure 12.2.8 shows the free-energy of solvation and energy contributions for the maltose dimer as a function of ψ calculated at φ=-30° and refers to the energy of the (-30°, 180°) conformer for two solvents, water and DMSO (Figure 12.2.8 a and b, respectively). In this section, the cavity term is a complex function of the size of the maltose molecule, as determined by the spatial orientation of the two glucose residues. The cavity energy is, by definition, always unfavorable; the more expanded the conformers, which are usually located in the low energy region of the map (around ψ=0° for maltose), the larger the G_{cav} due to the size of larger cavities to be created in the solvent.

The electrostatic free-energy, G_{el}, increases with the dipole and quadrupole moments of solute molecule and decreases with the radius of the cavity. On the other hand, the dipole moment μ is a function of dihedrals φ and ψ and for maltose has two large maxima around (φ, ψ)=(-40°,0°) and (180°, 140°) which is in agreement with the major contributions of G_{el} shown in Figure 12.2.8. The electrostatic free-energy (eq. [12.2.4]) is also dependent on the solvent dielectric constant and increases in passing from DMSO (ε=46.68 debye) to water (ε=78.30 debye) at 25°C. The dispersion term (eq. [12.2.5]) makes a significant contribution (-20 to -70 kJ·mol^{-1}) to the absolute value of solvation free-energy but the angular dependence is very small giving an almost equal contribution to the energy of conformers.

In an early paper[53] it was shown that, in the comparative cases of cellobiose and maltose, the probability distribution of conformers (Figure 12.2.9) is affected by the presence of the solvent, changing the shape of the function from one solvent to another. The minimum of the maltose map goes from (-20°,-30°) to (-10°,-20°) in water and DMSO, while that of cellobiose map goes from (0°, 50°) to (-30°, -20°) in both solvents.[53] These solvent perturbations (apparently small) on the conformational energies have a great effect on the proba-

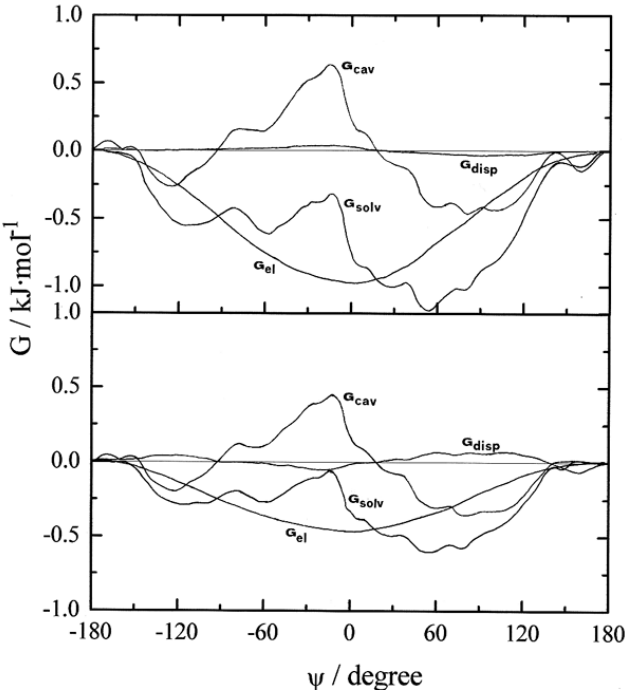

Figure 12.2.8. Section of the maltose energy map at φ=-30° showing the dependence of contributions to the G_{solv} as a function of angle ψ in water (a) and DMSO (b).

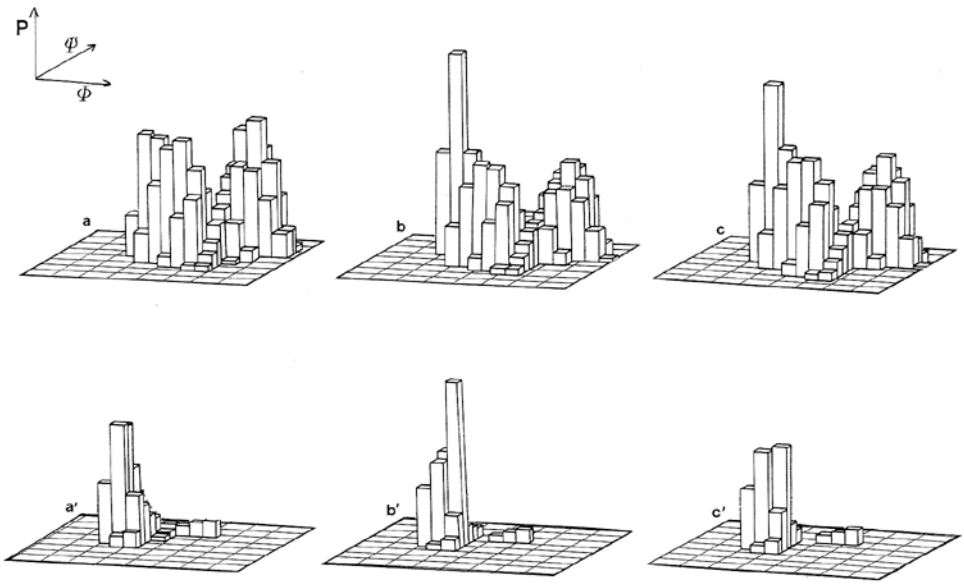

Figure 12.2.9. Histograms of probabilities of conformational states for cellobiose in vacuo (a), water (b) and DMSO (c), and for maltose (a', b', and c').

bilities associated with the conformers and therefore produce a rearrangement of statistical weights among conformers and, thus, a variation of the average properties of the system, as for example illustrated by the changes of the chain dimension parameters (see below Figure 12.2.11). Calculated average data like dipole moment, μ, linkage rotation, Λ, and proton-carbon coupling constants across glycosidic linkage, $^3J_{C1\text{-}H4}$ and $^3J_{C4'\text{-}H1}$, for β-D-maltose[14] and β-D-mannobiose[45] in different solvents are reported in Table 12.2.2. These results show that the equilibrium composition of dimer conformers depends strongly on the solvent and that the departure from the in vacuo conformation increases with increasing solvent dielectric constant. For mannobiose the determining factor of the solvent effect on the conformation is the intra-residue electrostatic interaction, which depends on φ and ψ in the same manner as the dipole moment.

Table 12.2.2. Calculated average values of dipole moment, four-bonds proton-carbon coupling constant and linkage rotation of β-D-maltose and β-D-mannobiose in different solvents at 25°C

Solvent	ε	φ, deg	ψ, deg	μ, debye	$^3J_{C1\text{-}H4}$, Hz	$^3J_{C4'\text{-}H1}$, Hz	Λ, deg
solute: β-D-maltose							
vacuum	-	-21	-28	3.80	4.2	4.5	-31
1,4-dioxane	2.21	-22	-22	3.89	4.1	4.5	-30
pyridine	12.40	-24	-39	4.02	4.0	4.5	-27
ethanol	24.55	-24	-41	4.09	3.9	4.5	-27
methanol	32.70	-25	-46	4.17	3.9	4.5	-25
DMSO	46.68	-24	-41	4.10	3.9	4.5	-28
water	78.30	-28	-65	4.47	3.7	4.7	-19
solute: β-D-mannobiose							
vacuum	-	81	-18	6.00	2.29	4.14	77
1,4-dioxane	2.21	82	-19	5.92	2.23	4.15	76
pyridine	12.40	91	-22	6.01	1.95	4.22	69
methanol	32.70	97	-24	6.08	1.72	4.25	54
DMSO	46.68	94	23	6.05	1.84	4.23	67
water	78.30	100	-18	6.27	1.53	4.32	57

It should be pointed out that even the small variations in the dihedral angles due to the presence of solvent molecules may produce a large change on a macromolecular scale, as discussed above.

12.2.4.2 Molecular dynamic methods

One of the most powerful theoretical tools for modeling carbohydrate solution systems on a microscopic scale and evaluating the degree of flexibility of these molecules is the molecular dynamics technique (MD) which has become popular over the last two decades. The first reported works of MD carbohydrate simulation appeared in 1986[54,55] and since then an in-

creasing number of MD simulations on sugars has been carried out.[11,13,56,57] The explicit representation of solvent molecules is required especially in biological systems, where solvent structuring plays an important role. Starting with an appropriate potential energy function for sugar-water interactions,[13,58] the common solution simulations are carried out by placing the solute molecule in the center of a cubic box of finite dimensions containing a given number of solute molecules which usually corresponds to at least three solvation shells.[11] The macroscopic system is then simulated by using the approximation known as "periodic boundary conditions",[59] in which the entire box is replicated in every direction, leaving solute and solvent molecules to interact with each other both in central and in replica boxes and setting the long-range interactions to smoothly decrease to zero by using the appropriate switching functions. A pair distribution function, g(r), defined as:

$$g(r) = \frac{1}{4\pi\rho r^2}\frac{dN(r)}{dr}$$

where:

r	interatomic distance
ρ	the bulk number density
N(r)	number of atoms of given type at distance r

has been used to evaluate the normalized probability of finding a water oxygen atom at a distance r from a given atom on the carbohydrate molecule.[11] In this way the anisotropic distribution of solvent molecules around carbohydrate solutes was reported[11,60,61] showing an exceptional structuring of water molecules which extends to greater distances around the solute as compared to the pure solvent. One of the most interesting results of these simulations is the identification of the spatial distribution of water molecules on the van der Waals' surface of the carbohydrate molecules. Figure 12.2.10 shows a probability density excess of the water molecules in a channel, which is effectively a bisector of the two closest sites for hydrogen bonding.

When the energy maps have been obtained by molecular mechanics calculations, dynamics simulations of disaccharides in various conformations are carried out to analyze the

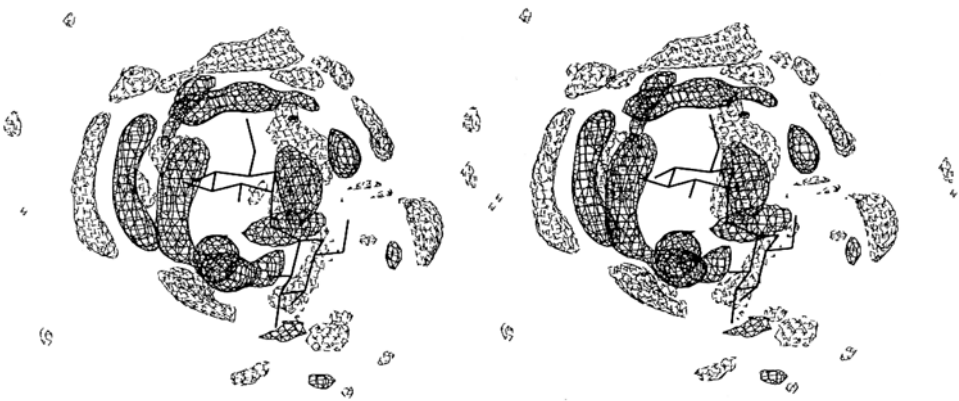

Figure 12.2.10. Contours of solvent anisotropic density around the α,α-trehalose disaccharide obtained from MD simulation [unpublished figure kindly provided by J.W. Brady and Q. Liu].

typical motions of the molecules along the conformational space at moderate temperatures. In general, initial conformations in the simulations are taken from one of those of minimized geometry as identified in the calculation of the energy map. Trajectories are then computed by assigning to the atoms velocity components randomly selected from a thermal distribution at a given temperature. By superimposing the trajectories of fluctuations of (φ, ψ) on the energy map, it is possible to observe a variety of motions, involving both the structures of the molecular rings and in some cases rotations about the glycosidic bonds and exocyclic torsions.[62] In the case of multiple minima, conformational transitions between low energy regions may also be revealed.

12.2.5 SOLVENT EFFECT ON CHAIN DIMENSIONS AND CONFORMATIONS OF POLYSACCHARIDES

In addition to the change of entropy, minimization of free energy in a binary dilute solution containing solvent and polymer occurs as a result of the favorable interactions between the chain segments and the solvent, which replace the homotactic interactions between solvent molecules and those between chain segments. In a good solvent and a very dilute solution, it is likely that only solute-solvent and solvent-solvent interactions prevail. However, in a bad solvent (and, in general, in a more concentrated solution) persistence of segmental interactions among chains is the major contribution in the macroscopic properties of the system. The theoretical evaluation of the entropic contributions arising from the configurational nature of the chain molecule is possible on the basis of thermodynamic-statistical models.[63] More troublesome is the contribution of enthalpy change of mixing, $\Delta_{mix}H$, of non-ionic polysaccharides and water which cannot be predicted, not even in sign. Furthermore, the scarcity of literature data does not allow any empirical rationalization although, in most cases, contributions significantly smaller than the related monomers are reported.

Notwithstanding the above limitations, a general picture can be drawn showing that the average dimension of a chain, experimentally obtained with light scattering or viscometric measurements, depends upon solvent interactions and behavior, in addition to the intrinsic features of the polysaccharide (chemical nature and linkage of monomers, conformational equilibria, etc.). The basic axiom is that solution properties are strictly related to the conformation of the molecules in the solvated state and this state, in turn, is only statistically defined from the primary (chemical) structure. In first instance, one can generalize the statement that non-ionic crystalline molecules and especially polymers, barely preserve their ordered conformation upon dissolution (Figure 12.2.2). Polymers and oligomers (including most carbohydrate molecules) generally assume a statistically disordered conformation in solution since, in the absence of specific favorable enthalpy contributions, polymer-solvent interactions provide a small increment in the entropy of mixing. Under these very common circumstances, the dissolution of a crystalline carbohydrate molecule, which is stabilized in the solid state by a great number of interactions, becomes a thermodynamically unfavorable event. Structurally speaking, the dissolution is made possible only by a sufficient increment in conformational entropy, which is described by the increment in conformational states accessible to the molecule.

In general, some conformational features, resembling those observed in the solid state, can be preserved also in solution (Figure 12.2.2), but the degree of order is strictly related to the presence of the solvent, in addition to the temperature and to the entropy of mixing. Figure 12.2.2 shows glucan chains with different types of linkages, and different pictorial trajectories which give different and sometimes surprising values of configurational entropy

are also observed. For example, those of (1-4)-linked α-D-glucan and of (1-3)-linked β-D-glucan seem fairly restricted to some pseudo-helical character compared to the more disordered set of trajectories that would be obtained if rotations about the glycosidic bonds were completely unrestricted. Possible interactions between residues of the polysaccharide chain that are not nearest-neighbors in the primary sequence of the polymer can sometimes be ignored. In this case, a computer-based polysaccharide chain can be constructed from the conformational energy map of the dimeric units. The Monte Carlo method[64] and the Flory matrix methods[65] are commonly used in the so-called "nearest-neighbors approximation" to mimic the polymer chains in the pure amorphous state or in dilute solution.

The Monte Carlo sample of chains reflects the range of conformations experienced by any single chain as a function of time or, equivalently, the range of conformations in a large sample of chemically identical polymer molecules at any instant in time. In either sense, the sample can be analyzed to deduce both the characteristics of individual chain conformations and the mean properties of the sample as a whole, which correspond to those in the equilibrium state of the chain. Results refer, however, to an "unperturbed" chain model that ignores the consequences of the long range excluded volume effect, because only nearest-neighbor interactions are accounted for.

Given a sufficient Monte Carlo sample of chains in equally probable representative conformations, it is possible to assess many mean properties of the polymer in question simply by computing numerical (unweighted arithmetic) averages over the number of chains in the sample. For example, the mean square end-to-end distance, the mean square radius of gyration, or the angular dependence of scattered light (particle scattering factor) are all mean geometric properties readily computed from a knowledge of the coordinates of the atoms or atomic groups which are generated in the Monte Carlo sample. The average topological properties are described through the chain-length dependence of quantities such as the characteristic ratio, C_n, the persistence length, P_n, and the correlation function, F_n, defined as:

$$C_n = \frac{\langle r^2 \rangle_0}{nL^2}, \quad P_n = \left\langle \left(\frac{\vec{L}_1}{L_1} \right) \sum_{i=1}^{n} \vec{L}_i \right\rangle_0, \quad F_n = \langle \vec{u} \vec{u}_n \rangle_0 \qquad [12.2.6]$$

where:

n	number of saccharide units
L	average virtual bond length
$\langle r^2 \rangle_0$	mean square end-to-end distance

The virtual bond vector is often defined for each monosaccharidic unit as connecting oxygen atoms involved in glycosidic linkages. Figure 12.2.11 shows the calculated properties of equations [12.2.6] for two homoglucan chains which differ only in the configuration of the anomeric carbon, i.e., (a) the $[\alpha\text{-D-(1-3)-glc}]_n$ (pseudonigeran) and (b) the $[\beta\text{-D-(1-3)-glc}]_n$ (curdlan). Whatever the chemical features, provided that the molecular weight is very large (that is for a degree of polymerization n which approaches infinity), the distribution of unperturbed polymer end-to-end length is Gaussian and C_n equals an asymptotic characteristic ratio C_∞, i.e.:

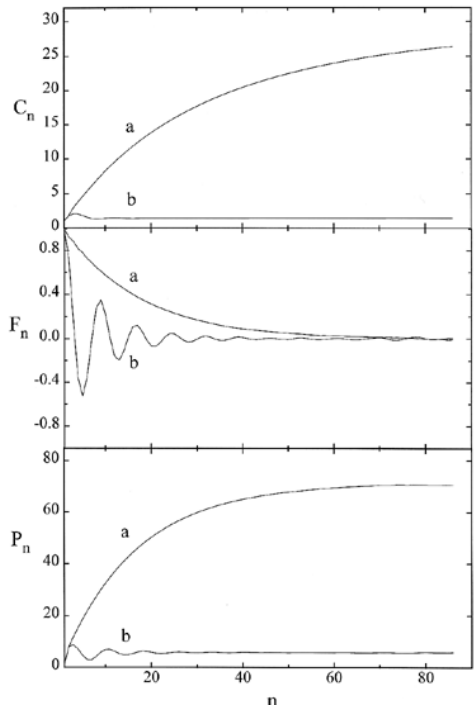

Figure 12.2.11. Characteristic ratio, correlation function and persistent length as a function of the degree of polymerization, n, for $[\alpha\text{-D-(1-3)-glc}]_n$ (pseudonigeran) and (b) the $[\beta\text{-D-(1-3)-glc}]_n$ (curdlan) calculated on the in vacuo energy maps.

$$C_\infty = \lim_{n\to\infty} \frac{\langle r^2 \rangle}{nL^2} = \frac{6\langle R_g^2 \rangle}{nL^2}$$

where R_g is the average square radius of gyration experimentally accessible. This relation is considered extremely important in the sense that any conformational perturbation is amplified by a factor n in the final value of C_∞ (or of $\langle R_g \rangle$), and therefore represents a highly demanding test for the appropriateness of the conformational calculations and at the same time a discriminating factor for conformation-dependent solution properties (e.g., viscosity).

An alternative measure of chain extension is the persistent length, P_n, which behaves in a similar asymptotic dependence on n as observed for C_n, in Figure 12.2.11. It is meant as the capacity of the chain to preserve the direction of the first residue (vector) of the chain. Therefore, as the directional persistence dissipates with increasing chain length and the direction of the terminal residue vector L_n loses correlation with that of the initial vector L_1, P_n approaches an asymptotic limit for sufficiently long chains. Both the C_n and P_n functions in Figure 12.2.11 reveal the $[\alpha\text{-D-(1-3)-glc}]_n$ chain to be much more extended than that of $[\beta\text{-D-(1-3)-glc}]_n$.

The directional correlations are also well characterized by the correlation function F_n of equations [12.2.6], which measures the average projection of a unit vector aligned with each virtual bond of the chain onto the unit vector relative to the first residue. The strongly oscillating character of F_n for $[\beta\text{-D-(1-3)-glc}]_n$, which is also observed at low n in both the C_n and P_n functions, reflects the pseudo-helical persistence of the backbone trajectory which becomes uncorrelated (i.e., F_n declines to zero) as the molecular weight increases. It is noteworthy that the oscillations in F_n retain approximately the pseudo-helical periodicity present in the crystalline forms of that polysaccharide (Figure 12.2.2). The monotonic decline of F_n (a) for $[\alpha\text{-D-(1-3)-glc}]_n$, on the other hand, shows that this polymer possess a stronger directional correlation due to the different glycosidic linkage which has a dramatic effect on the character of the chain trajectory.

The chain properties illustrated above are often described with terms such as “stiffness” and “flexibility”. It is important to clarify that stiffness and structural rigidity may not necessarily be alternative to flexibility and structural disorder, since two different concepts enter into the above definitions: one is concerned with the number of different accessible conformations, the other with the (average) direction of the sequential bonds, i.e., with the chain topology.

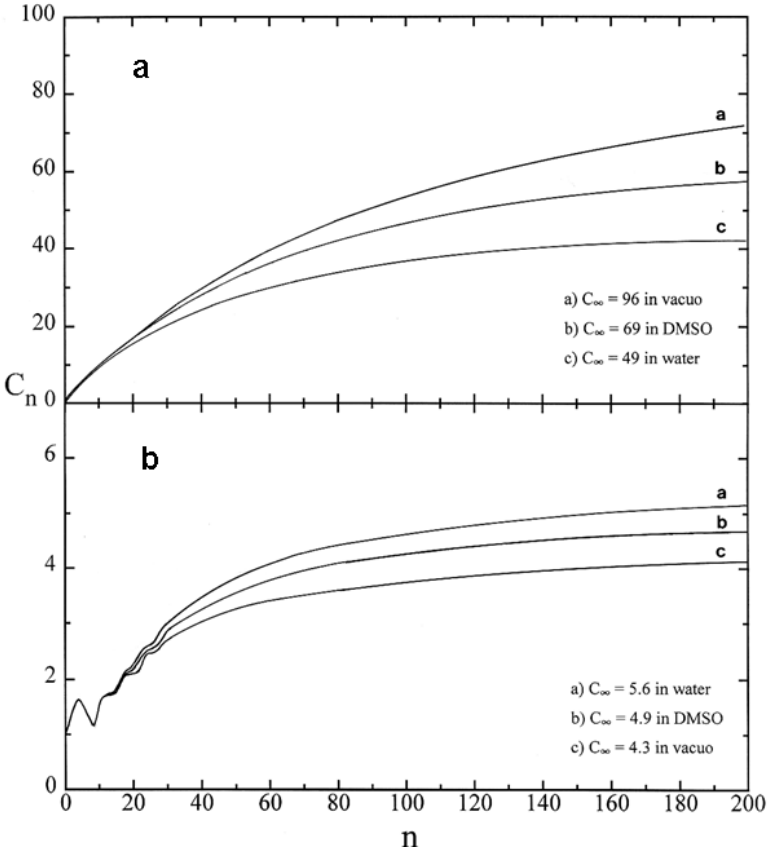

Figure 12.2.12. Characteristic ratio, C_n, as a function of degree of polymerization, n, for amylose (a) and cellulose (b) in vacuo, water and DMSO.

By calculating of the conformational energy surface of a dimer as a starting point for the prediction of mean chain properties, the effect of the solvation on the chain conformation is taken into account by evaluation of the perturbations of such surface due to the presence of the solvent. The characteristic ratio (eq. [12.2.6]) has been computed for (a) $[\beta\text{-D-(1-4)-glc}]_n$ (cellulose) and (b) $[\alpha\text{-D-(1-4)-glc}]_n$ (amylose) in different solvents, namely, water and DMSO.[53] The results are reported in Figure 12.2.12 where, for comparison, the in vacuo C_n for both polymers is shown. Figure 12.2.12a shows that the chain extension of cellulose decreases significantly in DMSO and much more so in water with a reduction of about 50% when compared to that in vacuo data (C_∞=96). The solvation contribution of water seems to favor those conformations, which have smaller cavity volumes and thus force the chain to minor extensions. Tanner and Berry[66] reported, for cellulose derivatives in solution, a value for the limiting characteristic ratio of between 30 and 60, which is in good agreement with the theoretical data in Figure 12.2.12a.

Figure 12.2.12b shows the characteristic ratio of amylose chains computed in the same solvents as in Figure 12.2.12a. The amylose chain extension is considerably lower than that of cellulose and, as in the case of $[\beta\text{-D-(1-3)-glc}]_n$ shown above, presents at low n a remark-

able pseudo-helical pattern. With respect to cellulose, the amylose chain shows a more coiled and apparently disordered backbone topology, but from a statistical point of view possesses a lower configurational entropy,[67] i.e., a more limited set of allowed conformational states. The C_∞ values are higher in water (5.6) than in DMSO (4.9) and both are higher than for the unperturbed chain which is in good agreement with the earlier work of Jordan and Brant[67] which observed a decrease of about 20% in chain dimensions of amylose DMSO/water mixture with respect to the water alone. More recently, Nakanishi and co-workers[68] have demonstrated from light scattering, sedimentation equilibrium and viscosity measurements on narrow distribution samples, that the amylose chain conformation in DMSO is a random coil, which results expanded ($C_\infty = 5$) by excluded-volume effect at high molecular weight. Norisuye[69] elaborated a set of published viscosity data reporting a $C_\infty = 4.2\text{-}4.5$ for unperturbed amylose and $C_\infty = 5.3$ for aqueous KCl solutions, while Ring and co-workers[70] estimated a $C_\infty \cong 4.5$ for amylose/water solutions by means of the Orofino-Flory theory of the second virial coefficient.

Order-disorder conformational transitions very often occur on changing physical and/or chemical conditions of polysaccharide solutions. DMSO, for example, is the solvent, which is commonly used as co-solvent for stabilizing or destabilizing ordered solution conformations. Schizophyllan, a triple helical polysaccharide with a $[\beta\text{-D-}(1\text{-}3)\text{-glc}]_n$ backbone exhibits a highly cooperative order-disorder transition in aqueous solution.[71] When small quantities of DMSO are added to aqueous solutions the ordered state is remarkably stabilized, as has been observed in the heat capacity curves by means of the DSC technique.[71]

Several efforts have been made with MD simulations in order to explicitly take into account the solvent molecule effect on the saccharide conformation, although only oligomeric segments have been considered, given the complexity in terms of computational time required for such a multi-atoms system. One interesting example is that of Brady and co-workers[56] on the stability and the behavior of double-helix carrageenan oligomer in aqueous solution compared with the results of the in vacuo calculations. They observed a higher relative stability of the double helix in vacuo, a fact, which is consistent with experimental results under anhydrous conditions, as in the fiber diffraction studies. However, in aqueous solution, the interchain hydrogen bonds that stabilize the double-helix structure appear much less stable, as the glycosidic hydroxyl groups make more favorable interactions with water molecules. They concluded that in the solvation step the double-helix would seem to be unstable and an unwinding process is theoretically predicted, at least for the oligomers.

12.2.6 SOLVENT EFFECT ON CHARGED POLYSACCHARIDES AND THE POLYELECTROLYTE MODEL

12.2.6.1 Experimental behavior of polysaccharides polyelectrolytes

Based on the experimental evidence of polyelectrolyte solutions, whenever the degree of polymerization is sufficiently high, all ionic macromolecules are characterized by a peculiar behavior, which sets them apart from all other ionic low molecular weight molecules as well as from non-ionic macromolecules. A general consequence of the presence of charged groups in a chain is a favorable contribution to the solubility of polymer in water. A strongly attractive potential is generated between the charge density on the polymer and the opposite charges in solution. For example, the value of the activity coefficient of the counterions is strongly reduced with respect to that of the same ions in the presence of the univalent opposite charged species. If the charge density of the polyelectrolyte is sufficiently high, such a

phenomenon is justified through a 'condensation process' of counterions and it has also been interpreted theoretically.

On the polymer side, among the dramatic changes that the presence of charged groups imparts to solution properties, there are the enhanced chain dimensions, the increased hydrodynamic volume (i.e., viscosity), and, in general, a strong influence on all conformational properties. Subject to the constraints imposed by the chemical structure of the chain, the distribution of charged groups and their degree of ionization contribute to determining the equilibrium chain conformation; both the Coulombic interaction among the charged groups and the distribution and concentration of the screening counterions are important. Most of the physico-chemical properties of the system result from a non-linear combination of these parameters.

However, one has not to forget that the variability of conformation alters the distances between charged groups on the polymeric chain and that the equilibrium is statistically defined by the Gibbs energy minimum of the system. As an important consequence of this energy balance, changes in temperature, ionic strength, pH, etc., can provoke changes in polyelectrolyte conformation, often cooperatively in the case of biopolymers, between states with different values of the charge density. These states may be characterized by different structural orders (e.g. helix $\rightarrow$ extended chain transition), by different degrees of flexibility of the chain (globular coil $\rightarrow$ expanded chain) or by different extent of aggregation (monomeric $\rightarrow$ dimeric or multimeric chains).

Theoretical calculations based on molecular grounds are still extremely complicated and incomplete[72] and other routes must be more empirically used in order to interpret the experimental data and to understand the correlation between conformational properties and structure. The central problem is to quantify the interactions among charges on the polymer and among these same charges and their respective counterions.

As far as it concerns the short-range interactions, the introduction of charged groups modifies the equilibrium geometry of the monomeric units and the contribution of the electrostatic nature on the nearest-neighbor conformational energy. These conclusions also derive from the already demonstrated effect of the solvent interactions on the unperturbed dimensions of amylose and cellulose,[53] and from the evidence of the perturbation on the conformational energy surface of several charged saccharidic units.[73]

There at least two approaches that may be relevant for this review; one is that described by Haug and Smidsrød[74] for the rationalization of the dimensional properties of polyelectrolytes as a function of salt concentration, the other is the formulation of a statistical thermodynamic theory for the "physical" framing of the ion-polyelectrolyte interactions. Both these theoretical formulations deal with the conformation of the polymer and predict that the conformational features must be function of ionic strength (see for example refs. 75 and 76).

12.2.6.2 The Haug and Smidsrød parameter: description of the salt effect on the chain dimension

A peculiarity of the correlation between the viscometric parameters and the dimensions of the macromolecular chain has long been recognized and theoretical approaches have been developed for several chain models.[77,78] The behavior of polyelectrolytes adds some complications especially in the low ionic strength regime. It has however been understood that the intrinsic viscosity, $[\eta]$, of a polyion (i.e., its hydrodynamic volume) decreases with increasing ionic strength, I, as a consequence of the screening of the fixed charges on the

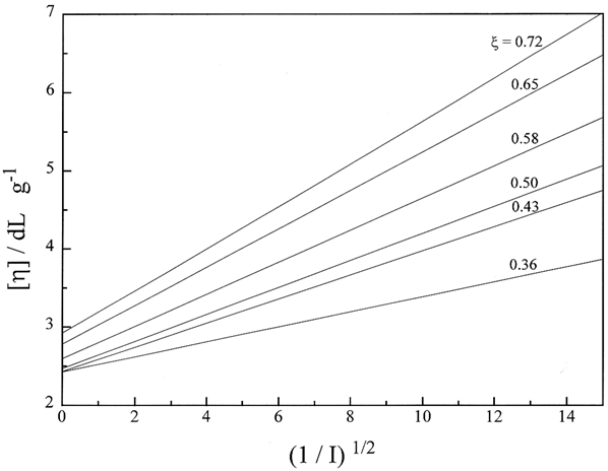

Figure 12.2.13. Dependence of the intrinsic viscosity [η] of hyaluronic acid (ξ=0.72) and its benzyl derivatives with decreasing linear charge density, ξ, on the inverse square root of ionic strength, I, at 25°C.

polyion. At infinite ionic strength, the chain dimensions may eventually correspond to the completely uncharged macromolecule. This is a sort of "ideal state" of the polyelectrolyte; "ideal" with respect to the long-range electrostatic repulsive interactions only, without relation to the Θ-conditions.

In the absence of a cooperative conformational transition, for many polysaccharide polyelectrolytes a linear dependence of [η] upon $I^{1/2}$ is observed, with the slope diminishing with the charge density associated to the polysaccharide chain (Figure 12.2.13). A theory has been presented for an estimation of the relative stiffness of the molecular chains by Smidsrød and Haug,[74] which is based on the Fixman's theory and Mark-Houwink equation. The chain stiffness parameter is estimated from the normalized slope B of [η] vs. the inverse square root of the ionic strength:

$$\frac{\partial[\eta]}{\partial I^{-1/2}} = slope = B\left([\eta]_{0.1}\right)^{\gamma} \qquad [12.2.7]$$

where:

γ has a value between 1.2 and 1.4

The dependence of viscosity on the ionic strength, as given in equation above, has been increasingly popular in the field of polysaccharides with the purpose of comparing the chain stiffness of different macromolecules. The derivation is based on the Fixman theory, which defines the dependence of [η] on the molecular weight through an expansion coefficient which effectively takes into account the electrostatic interactions in the Debye-Hückel approximation. The semi-empirical treatment of the hydrodynamic properties of statistical polyelectrolytes (at sufficiently high values of the ionic strength) is built upon a straightforward extension of the theory of intermolecular interactions for uncharged polymers, for which a linear relation can be written between the expansion coefficient, α_{η}^{3}, and the square root of the molecular weight, M. It should also be mentioned[78] that the various theoretical treatments of the salt dependence of the excluded volume and of the expansion coefficients

led to a linearity of α_η^3 on $(M/C_s)^{1/2}$ only over a limited range of salt concentration. On varying the salt concentration, one effectively deals with a set of binary solvents with a variety of interaction parameters. The approach proposed by Smidsrød overcomes the indetermination of some parameters by using the slope of [η] as a function of the inverse square-root of the ionic strength of the medium. The ultimate relationship is obtained between the constant B and the effective bond length b_θ ($B = \text{const} \cdot b_\theta^{-2}$), which, in the absence of any reasonable knowledge of the constant, can only be used in an empirical way.

There is a compelling although intuitive limit to the use of the Smidsrød-Haug approach for those macroions that do not counterbalance the effective electrostatic field exerted by the ionic strength through the conformational elasticity. Among these polymers, those characterized by a low value of fixed charges, of flexibility, and/or of molecular weight fall behind the limits of the correct applicability of the Smidsrød-Haug approach, which should maintain its validity only for gaussian chains with prominent electrostatic interactions. Most likely, the Smidsrød-Haug parameter has been abused in the field of polysaccharides without the authors' intention, in the sense that the original treatment was aware about the intrinsic limitations of the approach,[74] while the extensions have thereafter been considered as permitted. We wish to point out that the above comment does not imply the failure of the linearity of [η] with $I^{-1/2}$, but only a meaningless result for the values of b_θ obtained for low-charged polysaccharide polyelectrolytes. Reference can be made to two series of polysaccharides (chitosans and hyaluronans), which have been investigated in some detail for the specific application of the Smidsrød-Haug approach.[79,80]

12.2.6.3 The statistical thermodynamic counterion-condensation theory of Manning

Linear polyelectrolytes bear a charge distribution along the chain, properly neutralized by small ions of opposite sign. In the absence of added salt, it is reasonably assumed that the charge density (when sufficiently high) will increase the local stiffness of the chain because of the electrostatic repulsion. For this reason the linear polyelectrolyte is often regarded as a charged rod. Osawa has introduced the concept of a critical charge density on the polymer and described the ion- pairing of polyion and counterions as condensation. The model described here has been extensively used in previous papers of the authors[81] and described in the original papers by Manning.[82] Let here simply give a few comments on the physical basis of this model relevant to the present case.

The counterion condensation (CC) theory, largely developed by Manning, gives analytical solutions to evaluate the electrostatic potential around a linear polyelectrolyte, provided its conformation is regular and fixed. The rigidity of the polymer seems therefore to be both a prerequisite and a result of the molecular polyelectrolyte theory, and it has been thought to be not too far from reality in many cases.[82] The application of the above theory to experimental results has been carried out with the assumption that the charge distribution is structurally defined by the monomer repeat as derived from the solid state fiber diffractograms, although sometimes the fully stretched chain conformation has been taken (Figure 12.2.14). The original work of Manning's counterion condensation theory has provided an elegant tool for describing several properties of polyelectrolytes in terms of the structural parameter, ξ, which is unequivocally defined as $e^2/\varepsilon kTb$, where e is the value of the elementary charge, ε is the dielectric constant of the medium, k is the Boltzmann constant, T is the Kelvin temperature, and b is the distance between the projections of the fixed charges of the polyelectrolyte on its contour axis. In the case of monovalent ions, for all

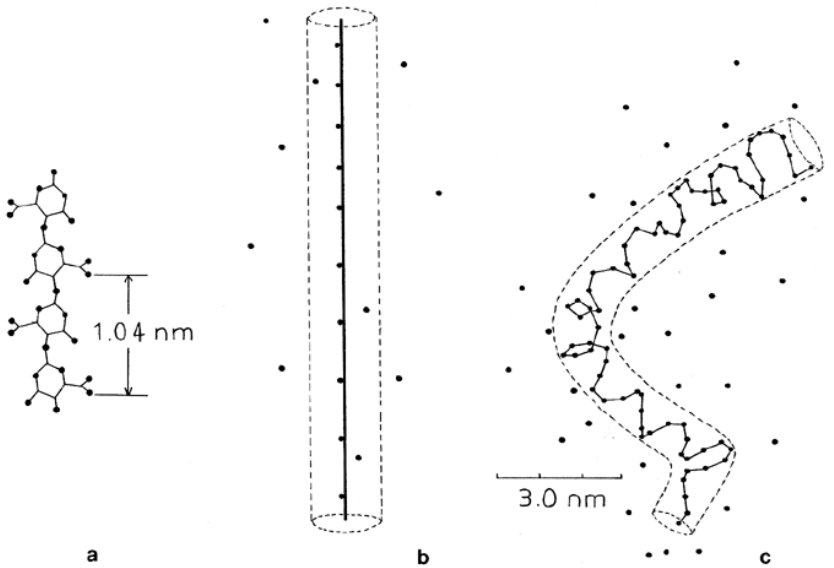

Figure 12.2.14. The rigid chain (a), the corresponding polyelectrolyte model (b) and the realistic flexible model of a polysaccharidic chain (c).

structural values of $\xi > 1$, a defined amount of counterions will "condense" from the solution into the domain of the polymer chain so as to reduce the "effective" value of ξ to unity. For water, $\xi = 0.714/b$ (with b expressed in nm), and is practically independent of T, being the electrostatic-excess Gibbs free energy of the solution given by:

$$G_{el} = -\xi \ln\left[1 - \exp(-Kb)\right]$$

where K is the Debye-Hückel screening parameter. Application of this theory has been made to many experimental cases, and in particular an extensive correlation has been made between the theoretical predictions and the thermodynamic data on the processes of protonation, dilution and mixing with ions.[76]

Besides these nice applications of the theory to problems with a strong "academic" character, there is another very striking example of prediction of solvent-induced conformational changes for the effects of salts on the conformational stability of ordered polyelectrolytes. In fact, in addition to the condensation phenomena predicted by the polyelectrolitic theory, other physical responses may also occur (also simultaneously), which may mask this central statement of the Manning theory "that the onset of the critical value ξ (for univalent ions $\xi > 1$) constitutes a thermodynamic instability which must be compensated by counterion condensation". In fact, chain extension and/or disaggregation of aggregated chains may occur or change upon the variation of charge density, and the energetic instability effectively becomes a function of the thermodynamic state of the polyelectrolytic chain.

The range of theoretical and experimental approaches has been, in particular, addressed to the problem of conformational transitions between two different states, provided they have different charge densities. For thermally induced, conformational transitions be-

tween states i and f of a polyelectrolyte, characterized by a set of ξ_i and ξ_f (i.e., b_i and b_f) values, polyelectrolyte theory predicts a simple relationship[82] between the values of the melting temperatures (T_M, the temperature of transition midpoint) and the logarithm of the ionic strength, I:

$$\frac{d\left(T_M^{-1}\right)}{d(\log I)} = -\frac{9.575F(\xi)}{\Delta_M H}$$

where $\Delta_M H$ is the value of the enthalpy of transition (in J per mole of charged groups) determined calorimetrically. This linearity implies, indeed, that the enthalpy change is essentially due to non-ionic contributions and largely independent of I. The function $F(\xi)$ depends on the charge density of both the final state (subscript f) and the initial state (subscript i), within the common condition that $\xi_f < \xi_i$, that is the final state is characterized by a smaller value of the charge density. The value of $F(\xi)$ is given in the literature.

This relation has been successfully applied first to the transition processes of DNA,[83] polynucleotides,[84] but also to many ionic polysaccharides (carrageenans,[85] xanthan,[86] succinoglycan,[87]) of great industrial interest. Accurate determination of the T_M values of the polysaccharide as a function of the ionic strength is necessary.

12.2.6.4 Conformational calculations of charged polysaccharides

The major problem for conformational calculations of ionic polysaccharides arises from the correct evaluation of the electrostatic potential energy due to the charged groups along the chain and to the all other ions in solutions. The interaction between the polyion charges and the counterions is formally non-conformational but it largely affects the distribution of the conformational states. Ionic polymers are often simplistically treated either in the approximation of full screening of the charged groups or in the approximation of rigid conformational states (regular rod-like polyelectrolyte models).

A combination of the molecular polyelectrolyte theory[82,83] with the methods of statistical mechanics can be used at least for the description of the chain expansion due to charges along the polysaccharide chain. The physical process of the proton dissociation of a (weak) polyacid is a good way to assess the conformational role of the polyelectrolytic interactions, since it is possible of tuning polyelectrolyte charge density on an otherwise constant chemical structure. An amylose chain, selectively oxidized on carbon 6 to produce a carboxylic (uronic) group, has proved to be a good example to test theoretical results.[81]

If the real semi-flexible chain of infinite length is replaced by a sequence of segments, the average end-to-end distance <r> of each segment defines the average distance <b> between charges:

$$\langle b \rangle = \frac{\langle r \rangle}{N} \qquad [12.2.8]$$

where N is the number of charges in the segment. The distance between charges fluctuates within the limits of the conformational flexibility of the chain, as calculated by the proper non-bonding inter-residue interactions.

The probability function W'(r) of the end-to-end displacement r of a charged segment can be obtained by multiplying its a priori (non-ionic) probability W(r) with the Boltzmann

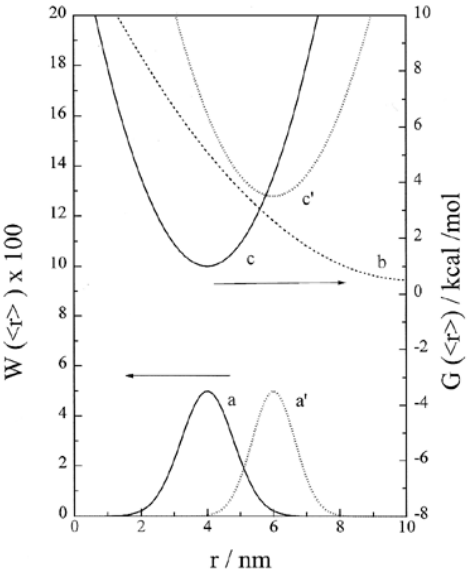

Figure 12.2.15. Dependence of the probability distribution function of a model semi-flexible chain, (a) uncharged and charged (a'), on the end-to-end distance and the respective total free energies (c and c'). The electrostatic contribution (b) is also reported.

term involving the excess electrostatic free energy (Figure 12.2.15). The probability theory guarantees both that the components (repeating units) of the segment vectors be distributed in a Gaussian way along the chain segment, and that high molecular weight polymers be composed by a statistical sequence of those segments. Consequence of the above approximation is that the distance r between any two points of the chain (separated by a sufficiently large number of residues, n) does not depend on the specific sequence and values of conformational angles and energies, but only upon the average potential summed over the number of residues n.

The calculation of the averaged (electrostatic) functions is reached in two steps. At the first, the proper flexibility of the polymer is evaluated either from conformational calculation or from suitable models, then the mean value of each property is calculated through the averaging procedure described below.

The computational procedure is the following:

- the conformational energy surface of the uncharged polymer is evaluated by the standard methods the conformational analysis;[65]
- the end-to-end distribution distance $W_n(r)$ for the (uncharged) polymer segments is determined by numerical Monte Carlo methods;[64]
- the dependence of the total (conformational) energy G(r) upon chain extension r is therefore estimated from the distribution of segment lengths; a Boltzmannian distribution is assumed.

In most cases the distribution function is Gaussian (or approximately so) and the corresponding free energy function can be approximated by a simple parabolic equation (Figure 12.2.15). In this case, we assume a Hookean energy (which is correct at least for the region around the maximum of the distribution curve), so we have:

$$W(r) = A\exp\left(-\frac{G}{RT}\right), \quad G(r) = k\left(r - r^0\right) \qquad [12.2.9]$$

where:

r^0	average segment length
k	a constant which determines the flexibility of the chain

The ionic energy, that results from the process of charging the polymer groups, changes the probability of the end-to-end distance for the i-th segment, W'(r), to the probability of the average inter-charge separation distance <b>, W(b), following the definition of equation [12.2.8] and [12.2.9].

The conformational (non-ionic) free energy, obtained from the radial distribution function for non-ionic chains by Monte Carlo calculations, was used in conjunction with the electrostatic free energy to calculate the actual distribution function of the charged chain segments. The resulting expansion justifies almost quantitatively in many cases the experimental thermodynamic properties (such as pK_a, H_{dil}, etc.) and the dimensional properties (viscosity) of the ionic polysaccharides to which the approach has been applied.

12.2.7 CONCLUSIONS

Only some aspects of the solvent perturbation on the conformational properties of carbohydrate polymers have been covered in this chapter. One of the major concerns has been to develop a description of these "solvent effects" starting with the complex conformational equilibria of simple sugars. In fact, only recently it has been fully appreciated the quantitative relationship between conformational population and physical properties, e.g. optical rotation.

The chapter, however, does not give extensive references to the experimental determination of the polysaccharide shape and size in different solvents, but rather it attempts to focus on the molecular reasons of these perturbations. A digression is also made to include the electrostatic charges in polyelectrolytic polysaccharides, because of their diffusion and use and because of interesting variations occurring in these systems. Thus, provided that all the interactions are taken into account, the calculation of the energetic state of each conformation provides the quantitative definition of the chain dimensions.

REFERENCES

1 J.R. Brisson and J.P. Carver, *Biochemistry*, **22**, 3671 (1983).
2 R.C. Hughes and N. Sharon, *Nature*, **274**, 637 (1978).
3 D.A. Brant, *Q. Rev. Biophys*., **9**, 527 (1976).
4 B.A. Burton and D.A. Brant, *Biopolymers*, **22**, 1769 (1983).
5 G.S. Buliga and D.A. Brant, *Int. J. Biol. Macromol.*, **9**, 71 (1987).
6 V. S. R. Rao, P. K. Qasba, P. V. Balaji and R. Chandrasekaran, *Conformation of Carbohydrates*, *Harwood Academic Publ*., Amsterdam, 1998, and references therein.
7 R. H. Marchessault and Y. Deslandes, *Carbohydr. Polymers,* **1**, 31 (1981).
8 D. A. Brant, *Carbohydr. Polymers,* **2**, 232 (1982).
9 P.R. Straub and D.A. Brant, *Biopolymers*, **19**, 639 (1980).
10 A. Cesàro in **Thermodynamic Data for Biochemistry and Biotechnology**, H.J. Hinz (Ed.), *Springer-Verlag*, Berlin, 1986, pp. 177-207.
11 Q. Liu and J.W. Brady, *J. Phys.Chem. B*, **101**, 1317 (1997).
12 J.W. Brady, *Curr. Opin. Struct.Biol.*, **1**, 711 (1991).
13 Q. Liu and J.W. Brady, *J. Am. Chem. Soc*., **118**, 12276 (1996).
14 I. Tvaroška, *Biopolymers*, **21**, 188 (1982).
15 I. Tvaroška, *Curr. Opin. Struct.Biol.*, **2**, 661 (1991).
16 K. Mazeau and I. Tvaroška, *Carbohydr. Res*., **225**, 27 (1992).
17 Perico, A., Mormino, M., Urbani, R., Cesàro, A., Tylianakis, E., Dais, P. and Brant, D. A., *Phys. Chem. B*, **103**, 8162-8171(1999).
18 K.D. Goebel, C.E. Harvie and D.A. Brant, *Appl. Polym. Symp.*, **28**, 671 (1976).
19 M. Ragazzi, D.R. Ferro, B. Perly, G. Torri, B. Casu, P. Sinay, M. Petitou and J. Choay, *Carbohydr. Res*., **165**, C1 (1987).
20 P.E. Marszalek, A.F. Oberhauser, Y.-P. Pang and J.M. Fernandez, *Nature*, **396**, 661 (1998).
21 S.J. Angyal, *Aust. J.Chem.,* **21**, 2737 (1968).
22 S.J. Angyal, *Advan. Carbohyd. Chem. Biochem*., **49**, 35 (1991).
23 D.A. Brant and M.D. Christ in **Computer Modeling of Carbohydrate Molecules**, A.D. French and J.W. Brady, Eds., ACS Symposium Series 430, *ACS*, Washington, DC, 1990, pp. 42-68.
24 R. Harris, T.J. Rutherford, M.J. Milton and S.W. Homans, *J. Biomol. NMR*, **9**, 47 (1997).
25 M. Kadkhodaei and D.A. Brant, *Macromolecules*, **31**, 1581 (1991).

26 I. Tvaroška and J. Gajdos, *Carbohydr. Res.,* **271**, 151 (1995).
27 F.R. Taravel , K. Mazeau and I. Tvaroška, *Biol. Res*., **28**, 723 (1995).
28 J.L. Asensio and J. Jimenez-Barbero, *Biopolymers*, **35**, 55 (1995).
29 P. Dais, Advan. Carbohyd. *Chem. Biochem*., **51**, 63 (1995).
30 F. Cavalieri, E. Chiessi, M. Paci, G. Paradossi, A. Flaibani and A. Cesàro, *Macromolecules*, (submitted).
31 I. Tvaroška and F.R. Taravel, *J. Biomol. NMR*, **2**, 421 (1992).
32 R.E. Wasylishen and T. Shaefer, *Can. J. Chem*., **51**, 961 (1973).
33 A.A. van Beuzekom, F.A.A.M. de Leeuw and C. Altona, *Magn. Reson. Chem*., **28**, 888 (1990).
34 I. Tvaroška, *Carbohydr. Res.*, **206**, 55 (1990).
35 I. Tvaroška and F.R. Taravel, *Carbohydr. Res*., **221**, 83 (1991).
36 J.P. Carver, D. Mandel, S.W. Michnick, A. Imberty, J.W. Brady in **Computer Modeling of Carbohydrate Molecules**, A.D. French and J.W. Brady, Eds., ACS Symposium Series 430, *ACS*, Washington, DC, 1990, pp. 267-280.
37 D. Rees and D. Thom, *J. Chem. Soc. Perkin Trans. II*, 191 (1977).
38 E.S. Stevens, *Carbohydr. Res*., **244**, 191 (1993).
39 D.H. Whiffen, *Chem. Ind*., 964 (1956).
40 J.H. Brewster, *J. Am. Chem. Soc*., **81**, 5483 (1959).
41 D. A. Rees, *J. Chem. Soc. B*, 877 (1970).
42 E.S. Stevens and B.K. Sathyanarayana, *J.Am.Chem.Soc*., **111**, 4149 (1989).
43 C.A. Duda and E.S. Stevens, *Carbohydr. Res*., **206**, 347 (1990).
44 R. Urbani, A. Di Blas and A. Cesàro, *Int. J. Biol. Macromol*., **15**, 24 (1993).
45. I. Tvaroška, S. Perez, O. Noble and F. Taravel, *Biopolymers*, **26**, 1499 (1987).
46 C. Gouvion, K. Mazeau, A. Heyraud, F. Taravel, *Carbohydr. Res*., **261**, 261 (1994).
47 R.A. Pierotti, *Chem. Rev*., **76**, 717 (1976).
48 R.J. Abraham and E. Bretschneider in **Internal Rotation in Molecules**, W.J. Orville-Thomas, Ed., *Academic Press*, London, 1974, ch. 13.
49 D.L. Beveridge, M.M. Kelly and R.J. Radna, *J. Am. Chem. Soc*., **96**, 3769 (1974).
50 M. Irisa, K. Nagayama and F. Hirata, *Chem. Phys. Letters*, **207**, 430 (1993).
51 R.R. Birge, M.J. Sullivan and B.J. Kohler, *J. Am. Chem.Soc*., **98**, 358 (1976).
52 I. Tvaroška and T. Kozar, *J. Am. Chem. Soc*., **102**, 6929 (1980).
53 R. Urbani and A. Cesàro, *Polymers*, **32**, 3013 (1991).
54 J.W. Brady, *J. Am. Chem. Soc*., **108**, 8153 (1986).
55 C.B. Post, B.R. Brooks, M. Karplus, C.M. Dobson, P.J. Artymiuk, J.C. Cheetham and D.C. Phillips, *J. Mol. Biol*., **190**, 455 (1986).
56 K. Ueda, A. Imamura and J.W. Brady, *J. Phys. Chem*., **102**, 2749 (1998).
57 R. Grigera, *Advan. Comp. Biol*., **1**, 203 (1994).
58 S.N. Ha, A. Giammona, M. Field and J.W. Brady, *Carbohydr. Res*., **180**, 207 (1988).
59 C.L. Brooks, M. Karplus, B.M. Pettitt, **Proteins: A Theoretical Perspective of Dynamics, Structure and Thermodynamics**, *Wiley Interscience*, New York, 1988, vol. LXXI.
60 R. Schmidt, B. Teo, M. Karplus and J.W. Brady, *J. Am. Chem. Soc*., **118**, 541 (1996).
61 Q. Liu, R. Schmidt, B. Teo, P.A. Karplus and J.W. Brady, *J. Am. Chem. Soc*., **119**, 7851 (1997).
62 V.H. Tran and J.W. Brady, *Biopolymers*, **29**, 977 (1990).
63 M. Karplus and J.N. Kushick, *Macromolecules*, **31**, 1581 (1981).
64 R.C. Jordan, D.A. Brant and A. Cesàro, *Biopolymers*, **17**, 2617 (1978).
65 P.J. Flory, **Statistical Mechanics of Chain Molecules,** *Wiley-Interscience*, New York, 1969.
66 D.W. Tanner and G.C. Berry, *J. Polym. Sci., Polym. Phys. Edn*., **12**, 441 (1974).
67 R.C. Jordan and D.A. Brant, *Macromolecules*, **13**, 491 (1980).
68 Y. Nakanishi, T. Norisuye, A. Teramoto and S. Kitamura, *Macromolecules*, **26**, 4220 (1993).
69 T. Norisuye, *Food Hydrocoll*., **10**, 109 (1996).
70 S.G. Ring, K.J. Anson and V.J. Morris, *Macromolecules*, **18**, 182 (1985).
71 T. Hirao, T. Sato, A. Teramoto, T. Matsuo and H. Suga, *Biopolymers*, **29**, 1867 (1990).
72 C. Sagui and T.A. Darden, *Ann. Rev. Biophys. Biomol. Struct*., **28**, 155 (1999).
73 J.R. Ruggiero, R. Urbani and A. Cesàro, *Int. J. Biol. Macromol*., **17**, 205 (1995).
74 O. Smidsrød and A. Haug, *Biopolymers*, **10**, 1213 (1971).
75 G.S. Manning and S. Paoletti, in **Industrial Polysaccharides**, V. Crescenzi, I.C.M. Dea and S.S. Stivala, Eds., *Gordon & Breach*, N Y, 1987, pp. 305-324.
76 S. Paoletti, A. Cesàro, F. Delben, V. Crescenzi and R. Rizzo, in **Microdomains in Polymer Solutions**, P. Dubin Ed., *Plenum Press*, New York, (1985) pp 159-189.

77 H. Morawetz, **Macromolecules in Solution**, *Interscience*, New York, 1975, Ch. 7.
78 M. Bohdanecký and J. Kovár, **Viscosity of Polymer Solutions**, *Elsevier*, Amsterdam, 1982, p. 108.
79 M.W. Anthonsen, K.M. Vårum and O. Smidsrød, Carbohydr. *Polymers*, **22**, 193 (1993).
80 R. Geciova, A. Flaibani, F. Delben, G. Liut, R. Urbani and A. Cesàro, *Macromol. Chem. Phys*., **196**, 2891 (1995).
81 A. Cesàro, S. Paoletti, R. Urbani and J.C. Benegas, *Int. J. Biol. Macromol*., **11**, 66 (1989).
82 G.S. Manning, *Acc. Chem. Res*., **12**, 443 (1979).
83 G.S. Manning, Quart. *Rev. Biophys.*, **11**, 179 (1978).
84 M.T. Record, C.F. Anderson and T.M. Lohman, *Quart. Rev. Biophys*., **11**, 103 (1978).
85 S. Paoletti, F. Delben, A. Cesàro and H. Grasdalen, *Macromolecules*, **18**, 1834 (1985).
86 S. Paoletti, A. Cesàro and F. Delben, *Carbohydr. Res*., **123**, 173 (1983).
87 T.V. Burova, I.A. Golubeva, N.V. Grinberg, A.Ya. Mashkevich, V.Ya. Grinberg, A.I.Usov, L. Navarini and A. Cesàro, *Biopolymers*, **39**, 517 (1996).